KARADENİZ TECHNICAL UNIVERSITY
THE GRADUATE SCHOOL OF NATURAL AND APPLIED SCIENCES

DEPARTMENT OF MECHANICAL ENGINEERING

FABRICATION AND CHARACTERIZATION OF POLYETHERSULFONE HOLLOW FIBER MEMBRANES

MASTER'S THESIS

Adil FAROOQ

JULY 2022
TRABZON

KARADENİZ TECHNICAL UNIVERSITY

THE GRADUATE SCHOOL OF NATURAL AND APPLIED SCIENCES

DEPARTMENT OF MECHANICAL ENGINEERING

FABRICATION AND CHARACTERIZATION OF POLYETHERSULFONE HOLLOW FIBER MEMBRANES

Adil FAROOQ

This thesis is accepted to give the degree of

"MASTER OF SCIENCE"

By

The Graduate School of Natural and Applied Sciences at
Karadeniz Technical University

The Date of Submission : **10 / 06 /2022**

The Date of Examination : **01 / 07 /2022**

Supervisor : **Assoc. Prof. Ömer Necati CORA**

Trabzon 2022

ACKNOWLEDGEMENT

The success of this work is attributed to Almighty God for his love, grace, favor, and kindness and for strengthening me throughout this research, and for giving me the knowledge to tackle and overcome the problems during my studies.

Appreciation to my supervisor, Associate Professor Ömer Necati CORA for his support, guidance, constructive criticism, immense encouragement, patience, full availability, and advice concerning this research and throughout the program. You give tutorship a whole new definition. You take it to heights that seem surreal yet real. Thanks for believing in me and providing all the support.

I would like to show my sincere gratitude to Associate Professor Dr. Recep GÜMRÜK for giving me advice from time to time. His dedication and keen interest to educate has inspired me to seek a career in academia. My thanks are also extended to the department's head in the person of Prof. Dr. Burhan ÇUHADAROĞLU.

To research assistants in persons of Doğan ACAR, and Mehmet SAĞLAM, I want to say a very big thank you for your collective effort in making the experimental campaign a success. Your support in every aspect is sincerely appreciated.

A special thanks to my Pakistani and Indian friends Jay, Athar, Faizan, Ovijit, Wajeeha, Yashfa, and most of all Farid. Farid has been like a mother to all of us, helping us whenever we need him. I appreciate whatever you have done for me.

To my close friends Zain, Glay, Merve, Eşma, Junaid, Swagga, and many others who am unable to name, thank you all for your support and unconditional love. To my brother from a different country Ridwan; If not for you, my life would have been much more difficult. Thank you for tolerating me.

A special thanks to Zeynep TÜRKER for always being ready to help me. You are the best Turkish language teacher that I could have asked for. If not for you, I wouldn't be able to speak Turkish so fluently.

My utmost appreciation goes to my mother Mrs. Abida FAROOQ for taking the role and responsibility of both a father and a mother – you are simply the best. To my sisters Shazia FAROOQ, and Heena FAROOQ, thanks for the trust and support that I feel wherever I go and whatever I do.

Adil FAROOQ

DECLARATION

This Master thesis, titled "Fabrication and Characterization of Polyethersulfone Hollow Fiber Membranes", which I, Adil FAROOQ presented as a Master's Thesis, was originally written by me and fully supported by my advisor, Assoc. Prof. Ömer Necati CORA, that I have gathered the data presented therein myself, that I have performed the experiments in the appropriate laboratory, that no results in this thesis have been fabricated, that I have fully documented the information I have obtained from other sources both in the text as well as the list of references, that I acted in compliance with scientific research and code of ethics during the research, and that no result from this thesis has been submitted/accepted for a degree at any other institution. In the event that the aforementioned declaration is violated, I accept full responsibility. 01/07/2022

Adil FAROOQ

TABLE OF CONTENT

ACKNOWLEDGEMENT III

DECLARATION IV

TABLE OF CONTENT V

ÖZET VIII

SUMMARY IX

LIST OF FIGURES X

LIST OF TABLES XII

ABBREVIATIONS XIII

1 INTRODUCTION 1

1.1 Importance of the Study 3

1.2 Scope of the Study 3

2 LITERATURE REVIEW 5

2.1 Introduction to Membranes 5

2.1.1 Historical Background of Hemodialysis Membranes 6

2.1.2 Terminology 8

2.2 Classification of Membranes 9

2.3 Membrane Fabrication Methods 11

2.3.1 Phase Inversion 11

2.3.2 Electrospinning 12

2.3.3 Track Itching 13

2.3.4 Sintering 14

2.4 Hollow Fiber Membrane Production by Phase Inversion 15

2.4.1 Phase Inversion Spinning Processes 17

2.4.1.1 Dry Spinning 17

2.4.1.2 Wet Spinning 17

2.4.1.3 Dry-jet Wet Spinning 18
2.4.1.4 Melt Spinning 18
2.5 Factors Affecting Fiber Characteristics 19
2.5.1 Polymer Type and Concentration 20
2.5.2 Type of Solvent 20
2.5.3 Type of Additives and Their Concentration 21
2.5.4 Bore Fluid 21
3 RESEARCH METHODOLOGY 22
3.1 Hollow Fiber Production Setup 22
3.1.1 Spinning Solution Delivery System 22
3.1.2 Bore Fluid Delivery System 23
3.1.3 Spinneret 24
3.2 Materials 25
3.3 Response Surface Methodology 26
3.4 Preparation of The Dope Solution 28
3.5 Hollow Fiber Membrane Fabrication 29
3.6 Post-treatment of The Fiber 31
3.7 Potting and Module Preparation 32
3.8 Membrane Characterization 33
3.8.1 Pure Water Permeability 33
3.8.2 Porosity 35
3.8.3 Scanning Electron Microscopy 37
3.8.4 Pore Size Distribution 38
4 RESULTS AND DISCUSSIONS 39
4.1 Determining The Spinning Solution Concentration Range 39
4.2 Spinning Conditions 40
4.3 Results of SEM, PWP and Porosity 40

4.4 Effect of Various Parameters on The Morphology of Membranes 43
4.4.1 Effect of Polymer Concentration on Morphology.....43
4.4.2 Effect of Additives on Morphology 44
4.4.3 Effect of Bore Fluid on Morphology 45
4.4.4 Effect of Air Gap on Morphology.....47
4.5 Effect of Various Parameters on Pure Water Permeability 48
4.6 Effect of Various Parameters on Porosity of The Produced Samples 55
4.7 Pore Size Variation.....60
5 CONCLUSIONS AND RECOMMENDATIONS 63
5.1 Conclusions 63
5.2 Recommendations 64
6 REFERENCES.....66
CURRICULUM VITAE

Yüksek Lisans Tezi

ÖZET

POLİETER SÜLFON İNCE BOŞLUKLU MEMBRANLARIN ÜRETİMİ VE KARAKTERİZASYONU

Adil FAROOQ

Karadeniz Teknik Üniversitesi
Fen Bilimleri Enstitüsü
Makine Mühendisliği Anabilim Dalı
Danışman: Doç. Dr. Ömer Necati CORA
2022, 70 Sayfa

Membran teknolojisi, su arıtma, tıp, biyoteknoloji, gıda, içecek ve metalurjik ayırma gibi bir çok proseste kullanılmaktadır. Bu çalışmada, polietersülfon (PES) ve gözenek oluşturucu polivinilpirolidon (PVP) (K30 ve K90) ile ince boşluklu fiber membranların üretilmesi ve karakterize edilmesi amaçlanmıştır. Bu hedeflere ulaşmak için küçük ölçekli bir elyaf membran üretim düzeneği tasarlanmış ve imal edilmiştir. Ardından, Box-Behnken deney tasarımı (DOE) ile dört bağımsız girdi değişkeni (polimer konsantrasyonu, ek moleküler ağırlık, delik içi sıvısı bileşimi ile hava ile temas mesafesi) ve bağımlı çıktı değişkenleri (morfoloji, membran çapı, membran kalınlığı, saf su geçirgenliği, gözeneklilik, gözenek boyutu dağılımı) dikkate alınarak bir deney planı oluşturulmuştur. N, N-Dimetilformamide (DMF) çözücü olarak kullanılmıştır. Su ve % 96'lık etanol çözeltisi iç katılaştırıcı sıvısı olarak kullanılmıştır. Sonuç olarak; artan polimer konsantrasyonu ile membranların PWP'si azalmıştır. %17 'lik polimer konsantrasyonunda en düşük geçirgenlik 24.8 l/m^2.s.bar' ken, en yüksek geçirgenlik değeri %11 'lik polimer konsantrasyonunda 452.2 l/m^2.s.bar olarak tespit edilmiştir. Taramalı elektron mikroskobu analizleri K90 içeren gözenek oluşturucu katkılı membranlarda süngerimsi morfolojileri ortaya çıkarmıştır. Katılaştırıcı sıvı olarak su kullanımı, sütün şeklindeki hücre yapılarına yol açarken, katılaştırıcı olarak su ve alkol karışımları, değişen derecelerde gözenek boyutlarına sahip süngerimsi yapılar oluşturmuştur. Gözeneklilik değerleri %.46,6 - %72,2 arasında değişiklik göstermiştir. Polimer oranının artması, gözenekliliğin azalmasına neden olurken, katkı maddesi oranının artması gözenekliliğin artmasına yol açmıştır. Ortalama gözenek boyutları ve dağılımları, geniş bir dağılım göstermiştir. En yüksek saf su geçirgenliğine (PWP) sahip membranın ortalama gözenek boyutlarının, en düşük PWP'ye sahip membrandan 10 kat daha büyük olduğu tespit edilmiştir.

Anahtar Kelimeler: Hemodiyaliz, polietersulfone membran, filtrasyon, ince boşluklu fiber membran, hemodiyaliz membran, kan saflaştırma.

Master's Thesis

SUMMARY

FABRICATION AND CHARACTERIZATION OF POLYETHERSULFONE HOLLOW FIBER MEMBRANES

Adil FAROOQ

Karadeniz Technical University
The Graduate School of Natural and Applied Sciences
Mechanical Engineering Graduate Program
Supervisor: Assoc. Prof. Ömer Necati CORA
2022, 70 Pages

Membrane technology is employed in a variety of industries because of its versatility such as water treatment, petrochemical, medical, and biotechnological, beverages, food, and metallurgical separation processes. The current study aims to produce and characterize hollow fiber membranes from polyethersulfone (PES) and pore former polyvinylpyrrolidone (PVP) . To achieve these goals, a small-scale hollow fiber membrane production setup was designed. Box-Behnken design of experiment (DOE) was then used to understand the relationship between four independent input variables (polymer concentration, additive molecular weight, bore fluid composition, and the air gap) and the dependent output variables (morphology, membrane diameter, membrane thickness, pure water permeability, porosity, and pore size distributions). N, N-Dimethylformamide (DMF) was used as the solvent. Water and ethanol (96%) were used as bore fluids. It was revealed that the pure water permeability (PWP) of the membranes was reduced with increasing polymer concentration. The lowest permeability found was 24.8 L/m^2.h.bar at 17% polymer concentration while the highest permeability value found was 452.2 L/m^2.h.bar at 11% polymer concentration. SEM analysis of the fiber membranes revealed spongy morphologies for membranes containing K90 pore former additive. Water as a quenching medium produced intrusion cells while water and alcohol combinations produced spongy structures with varying degrees of pore sizes. The porosity results varied in the range of 46.6-72.2%. Increasing the polymer content results in a reduction of porosity while increasing the additive concentrations increases the porosity. The average pore sizes and their distribution showed a large operational range. The average pore sizes of the membrane with the highest PWP were 10 times larger than the membrane with the lowest PWP.

Key Words: Hemodialysis, polyethersulfone membranes, filtration, hollow fiber membranes, hemodialysis membranes, blood purification.

LIST OF FIGURES

Page No

Figure 1.1. Working principle of hemodialysis 2
Figure 2.1. Schematic of the first rotating drum dialyzer during 1940's 6
Figure 2.2. Coil dialyzer developed in 1956 7
Figure 2.3. Kiil Dialyzer from 1960's 8
Figure 2.4. Dead-end Hollow fiber module 9
Figure 2.5. Different classification of membranes 10
Figure 2.6. A single-ion irradiation setup 13
Figure 2.7. Different pore shapes obtained during track itching 14
Figure 2.8. Membrane morphology based on demixing rates adopted from reference 16
Figure 2.9. Hollow fiber spinning processes 19
Figure 3.1. Schematic of the spinning solution delivery mechanism. 22
Figure 3.2. Spinning solution delivery system. 23
Figure 3.3. Bore fluid delivery system. 23
Figure 3.4. Schematic of the designed spinneret 24
Figure 3.5. Diagram of the spinneret used in hollow fiber production 24
Figure 3.6. Polyethersulfone chemical structure. 25
Figure 3.7. PVP chemical structure 25
Figure 3.8. Magnetic stirrer used for producing the dope solution 28
Figure 3.9. Vacuum chamber to remove residual air bubbles in the dope solution. 29
Figure 3.10. Schematics of the hollow fiber production setup 30
Figure 3.11. Hollow fiber spinning setup. 30
Figure 3.12. Flow of the dope solution through the spinneret. 31
Figure 3.13. Water post-treatment of hollow fiber membranes. 31
Figure 3.14. Schematics of the potted hollow fiber module. 32
Figure 3.15. Hollow fiber membrane module preparation 33
Figure 3.16. Schematics of the hollow fiber PWP test setup 34
Figure 3.17. PWP test setup 35
Figure 3.18. Weight of dry and wet membranes using precision a weighing scale. 36
Figure 3.19. ZEISS EVO scanning electron microscope (SEM). 37
Figure 3.20. Samples attached on the mount. 37
Figure 3.21. SPI gold sputter coater used to coat membrane samples for SEM 38

Figure 4.1. SEM images of the 27 membrane samples 41
Figure 4.2 Variation of pore size with polymer concentration. 44
Figure 4.3 Effect of additive molecular weight on PES morphology. 45
Figure 4.4 Effect of Water on the morphology of PES membranes. 46
Figure 4.5 Change in morphology with variation in bore fluid. 47
Figure 4.6 Variation of wall thickness and inner skin layer with the air gap. 48
Figure 4.7. 3-dimensional response surface plot for pure water permeability 50
Figure 4.8. Contour plot of the variation of PWP 51
Figure 4.9. Change in PWP with PVP molecular weight. 53
Figure 4.10. Visual representation of the significance of various spinning factors on PWP…… ….55
Figure 4.11. 3-dimensional response surface plot for porosity in response to 56
Figure 4.12. Contour plot of the variation of porosity responses 57
Figure 4.13. Visual representation of the significance of various spinning factors on porosity. 59
Figure 4.14. Pore size comparison between sample E5 and E16. 60
Figure 4.15. Average pore size distribution along the radius of sample E25. 61
Figure 4.16. Average pore size distribution graph of sample E25. 62

LIST OF TABLES

Page No

Table 3.1. Box-Behnken design methodology for the experiments 26

Table 3.2. Box-Behnken design matrix 27

Table 4.1. Trial recipes used for optimization 39

Table 4.2. Values of the controlled parameter 40

Table 4.3. PWP and Porosity test results. 42

Table 4.4. ANOVA output of the quadratic model for PWP. 53

Table 4.5. Model summary of R^2 54

Table 4.6. ANOVA output of the quadratic model for the porosity 58

Table 4.7. Model summary of R^2 for porosity 59

Table 4.8. Pore size comparison between samples E5 and E16. 61

LIST OF ABBREVIATIONS

BSA	Bovine Serum Albumin
DMA	Dimethylacetamide
DMF	N, N-dimethylformamide
HFM	Hollow fiber membrane
NF	Nanofiltration
PES	Polyethersulfone
PS	Polysulfone
PVDF	Polyvinylidenediflouride
PVP	Polyvinylpyrrolidone
PWP	Pure Water Permeability
SEM	Scanning Electron Microscope
UF	Ultrafiltration

1. INTRODUCTION

The human body is a complex organization of individual cells, tissues, organs, and organ systems. In the case of a healthy human being, these organs and organ systems function in complete harmony with each other. Malfunctioning of any one of the organs or organ systems disrupts the life processes of our bodies. The purification of blood by kidneys is one such example. The human kidneys are a pair of bean-shaped organs about 5 inches long. They are located below the rib cage behind the belly. Their chief function is to remove the wastes from the body in the form of urine. They also help in controlling body fluid levels. Like any other organ in our body, kidneys are susceptible to failure. Kidneys are one of the vital organs of our bodies, their failure can be fatal. Therefore, the health of kidneys is of utmost importance for healthy human being. Patients with end-stage kidney failure need dialysis to filter the wastes out of their bodies. The stages of kidney failure are determined by the Glomerular Filtration Rate (GFR). Table 1.1 shows the various stages of kidney failure.

Table 1.1 Stages of the loss of kidney function [1].

	Stages Of Chronic Kidney Diseases	**GRF (% of Kidney functionality)**
Stage 1	Damage to the kidneys without a functional loss	> 90
Stage 2	Damage to the kidneys and a slight reduction of renal function	89 to 60
Stage 3a	Mild to moderate renal function loss	59 to 45
Stage 3b	Modest to significant renal function loss	44 to 30
Stage 4	Severe renal function loss	29 to 15
Stage 5	Renal failure	Less than 15

Diabetes has been reported as the most popular cause of End-Stage Renal Disease (ESRD) followed by hypertension [1]. Other causes include autoimmune diseases (Lupus, etc.), glomerulonephritis, interstitial nephritis, etc. [2]. Patients with end-stage kidney failure

(GRF less than 15) either need a kidney transplantation (which is very difficult) or start dialysis. When the latter is considered, hemodialysis and peritoneal dialysis are the most popular types of dialysis.

Hemodialysis is a procedure in which blood is pumped out of the body and cleaned in a hemodialysis machine (Figure 1.1). The frequency of hemodialysis varies based on the severity of the condition. If performed at a center, it usually takes 3-5 hours, 3 times a week. However, people who do dialysis at home, on the other hand, can do it for 1-2 hours every day.

Peritoneal dialysis, on the other hand, involves inserting a catheter into the patient's belly through surgery. A dialysate is then injected into the body through this catheter. The peritoneum (the lining of the abdomen), which works as a natural filter, cleans the blood. After the filtration process is over, the fluid is removed from the body via the same catheter.

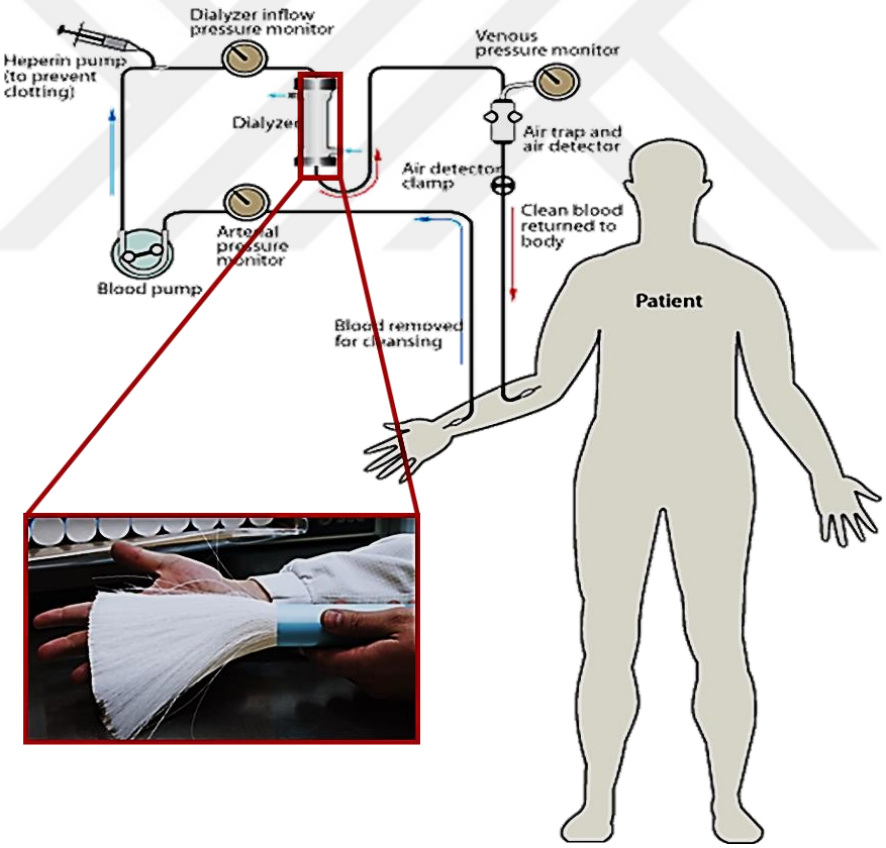


Figure 1.1. Working principle of hemodialysis, and the detailed view of hollow fiber membranes in dialyzer, After [3].

The goal of this thesis was set as fabrication and characterization of hollow fiber membranes that are similar to the ones used in hemodialysis processes.

1.1. Importance of the Study

In 1990, according to the Global Burden of Disease study, acute kidney failure was listed as the 27th cause of death around the world. However, in 2010, chronic kidney failure jumped to the 18th spot [4]. Around 750,000 people are affected by kidney failure in the United States alone every year and an estimated two million people, globally [5]. According to the 2020 report of The Turkish Journal of Nephrology, the number of hemodialysis patients is rising at an alarming rate. According to the report, in 2018, an estimated 81,055 patients received renal replacement therapies in Turkey and 74.8% of them were via hemodialysis [6]. If one considers the cost of a single hemodialyzer membrane to be in the range of $ 3-5 and each dialyzer is used only once, the cost of just the hemodialyzers is about $28.5-47.4 million dollars just for the year 2018.

In terms of hemodialysis membrane production, German company Fresenius produces more than half of the world's dialysis membranes [7]. The details of the processes and materials used in the production of hemodialysis membranes are mostly protected by copyright issues. The current study will try to fill this gap by investigating the morphology and other properties of such fiber membranes.

1.2. Scope of the Study

Whilst membrane technology has been around since the 1960s, and the technology first started to be used in different filtration processes like wastewater reclamation, blood purification, etc. The production of hollow fiber membranes with the desired morphological properties is a combination of art and science involving a wide spectrum of independent parameters.

The objective of the current study is to produce and characterize polyethersulfone (PES) hollow fiber membranes produced under different process conditions. To achieve these goals, a small-scale hollow fiber membrane production setup was designed. Box-Behnken design of experiment (DOE) statistical tool was used to understand the relationship between four independent input variables (polymer concentration, additive molecular weight, bore fluid composition, and the air gap) and the dependent output variable

(morphology, membrane diameter, membrane thickness, pure water permeability, porosity, and pore size distributions). The thesis included a detailed review of the literature on hollow fiber membrane fabrication, as well as the results of current study and recommendations for future research.

2. LITERATURE REVIEW

2.1. Introduction to Membranes

The last few decades have witnessed a rapid growth in membrane separation methods. Different membrane separation methods are of tremendous commercial interest, with a variety of applications in fields like bioseparation, water purification, wastewater treatment, etc. Hence, it has attracted attention, particularly in the field of separation technology. The hollow fiber membranes were first developed in the 1960s by Dow Chemicals. When compared with a flat sheet, tubular, or spiral wound membrane, hollow fiber membranes are superior because of the following advantages: 1) Higher efficiency due to increased surface area per unit volume 2) Comparatively easier to prepare, clean, and handle 3) It doesn't need any mechanical support [8]. This enabled the use of hollow fiber membranes in various commercial fields such as the medical field (hemodialysis, blood fractionation), water recycling (purification and desalination), ultrafiltration, microfiltration, reverse osmosis, gas separation, and so on [9]. Hollow fiber membranes are also used in membrane bioreactors (MBRs) that combine biological treatment with membrane separation. It has become an essential approach for municipal and industrial wastewater treatment [10]. State-of-the-art hollow fiber membrane contactors (MCs) have recently gained popularity as powerful devices for completing separation processes such as gas absorption and liquid-liquid extraction [11].

A membrane may be defined as a thin layer of semi-permeable material that is used for solute separation as transmembrane pressure is applied across it [12]. In human bodies, the same membrane referred to as bio-membrane performs the same function of selectively allowing materials into and out of the cells. Scientists are constantly looking for materials that can mimic and even replace bio-membranes with minimal rejection from the human body. The materials that show compatibility with human bodies with minimal rejection are called biomaterials. Any systemically, pharmacologically inactive substance or combination of substances used for implantation within or incorporation with a biological system to complement or replace activities of live tissues or organs is referred to as a biomaterial [13]. The hemodialysis membrane used in dialyzers is one of the many examples of a biocompatible material. These membranes are used to remove the metabolic wastes from the bodies of patients with end-stage renal disease (ESRD) [14].

2.1.1. Historical Background of Hemodialysis Membranes

Over the past century, more than twenty different hemodialysis machines have been developed. Even though literature regarding dialysis procedures date back to the 19th century from Scottish chemist Thomas Graham, who later came to be known as the "Father of Dialysis", yet the actual development in the field started in 1945 when Willem Kolff of the Netherlands introduced a machine called the rotating drum kidney (Fig. 2.1) using cellophane membranes and an immersion bath to treat a 67 years old patient with acute renal failure [15,16]. The limitations of this device included low transmembrane pressures (TMPs) resulting in limited ultrafiltration capabilities, and large extracorporeal blood volumes (a lot of blood was taken out of the body at a particular instant; about 500-700ml) [17].

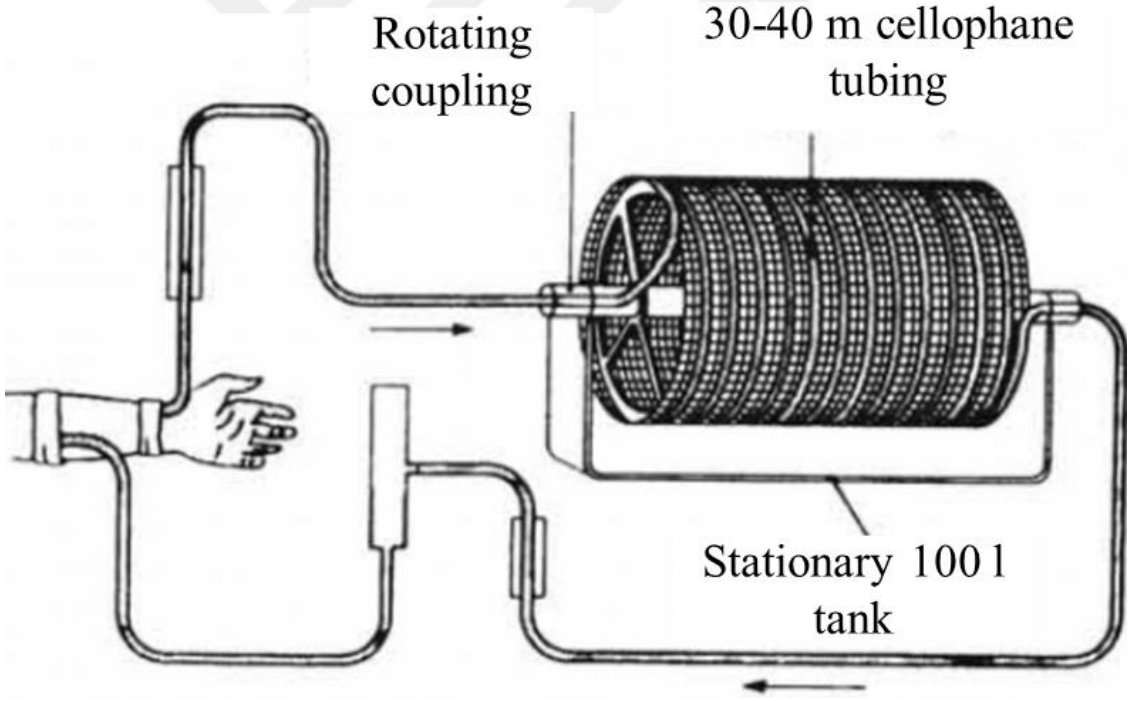


Figure 2.1. Schematic of the first rotating drum dialyzer during 1940's [18].

Another widely used dialyzer was the coil dialyzer (Figure 2.2). It was commercially launched in 1956 and comprised of a tubular membrane placed between flexible supports wrapped around a rigid cylindrical core. A recirculating volume of dialysate was delivered to the functional unit of this dialyzer (cellophane tubing surrounded by fiberglass). The

geometry of the dialyzer was such that it produced high compartment resistances resulting in high TMPs [14].



Figure 2.2. Coil dialyzer developed in 1956 [18].

In 1960, a new dialyzer (later called Kiil dialyzer) was developed under the supervision of Frederic Kiil, a urologist. This dialyzer used a few (three or more) boards with two or more sheets of membranes sandwiched between each pair of boards (Figure 2.3). The membranes are put between the boards, which are constructed of polypropylene. The boards are held in place by a sturdy frame. The board is protected by a gasket around its perimeter to prevent blood and dialysate from leaking. The membranes were made of more permeable cuprophan [19]. The initial designs of the Kiil dialyzers were not disposable, later on, multiple-use and disposable versions were made.

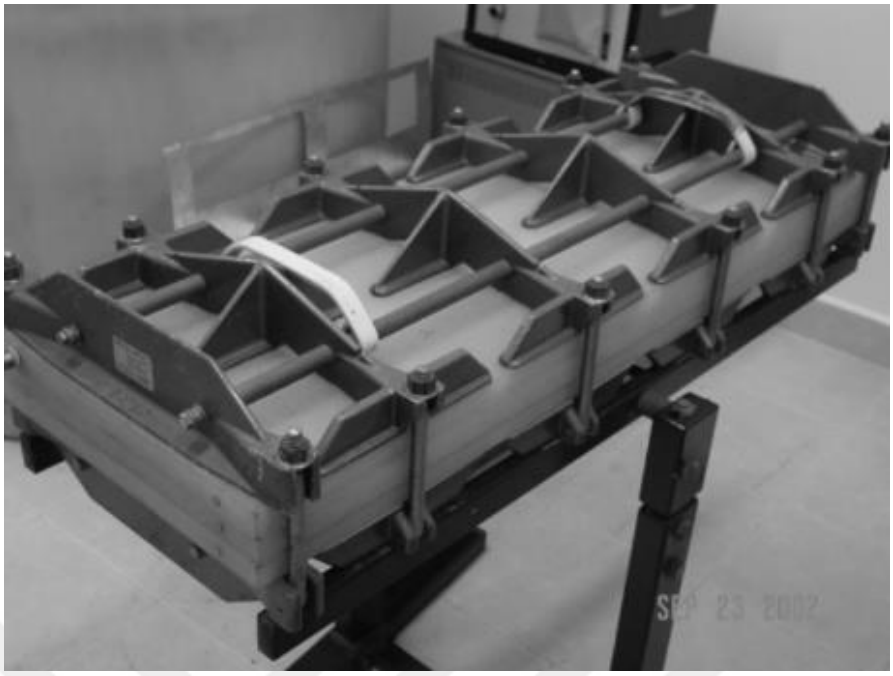


Figure 2.3. Kiil Dialyzer from 1960’s [19].

There were other types of dialyzers developed during that time, as well but all of them had many limitations, the most prominent ones being the high blood compartment volumes required, and inefficient mass transfer characteristics. These problems led to the development of hollow-fiber artificial kidneys in late 1960s.

2.1.2. Relevant Terminology

- Membrane: A membrane is a structure with lateral dimensions significantly larger than its thickness that allows specific materials to be transferred under a range of driving forces.
- Microfiltration: It is a membrane-based separation process performed under pressure that rejects particles and dissolved macromolecules larger than 0.1 µm.
- Ultrafiltration: It is a membrane-based separation process performed under pressure that rejects particles and dissolved macromolecules whose sizes are less than 0.1 µm and more than 2 nm.
- Nanofiltration: It is a membrane-based separation process performed under pressure that rejects particles and dissolved macromolecules whose sizes are less than 2 nm.

- Permeate: Permeate is the part of the fluid stream that passes through the membrane (Figure 2.4). The particles that passed through the membrane are called penetrants.
- Retentate: It is the part of the fluid stream that could not pass through the membrane and is devoid of penetrants (Figure 2.4).
- Coagulant: Coagulant is defined as a substance that induces coagulation in liquids or sols.
- Air Gap: It is the space between the coagulation bath and the spinneret outflow orifice.

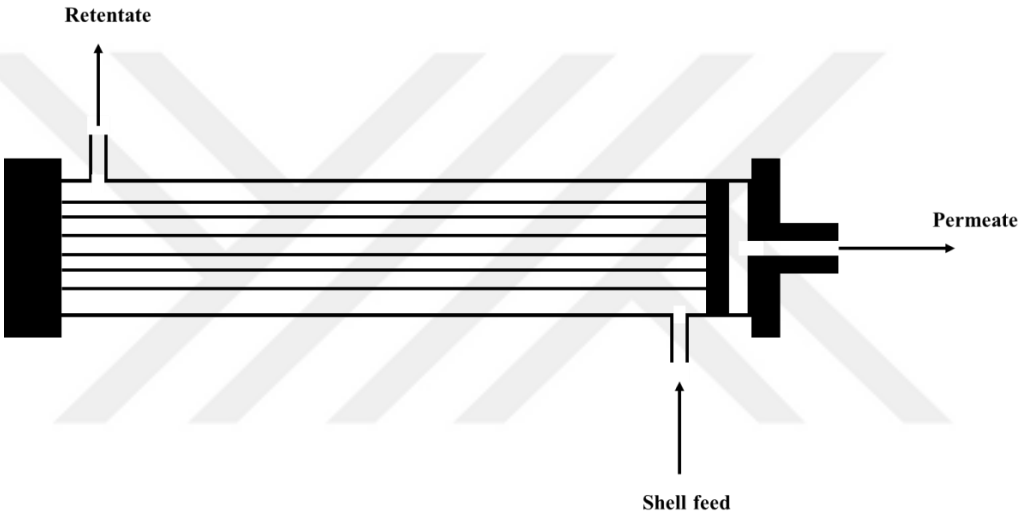


Figure 2.4. Dead-end hollow fiber module

- Module: A module is the assembly of the membranes to demarcate feed, permeate, and retentate (Figure 2.4).
- Flux: It can be defined as the flow rate of the permeate from the feed per unit area per hour. It is expressed as l/m^2h.

2.2. Classification of Membranes

Membranes can be classified into different groups based on their material, morphology, filtration, type, and driving force. Figure 2.5 shows the schematics of the membrane classification based on different factors.

Based on the level of filtration desired, membranes can be classified as ultrafiltration (UF), microfiltration (MF), Nanofiltration (NF), and reverse osmosis (RO). The only difference between them is the size (molecular weight) of the particles that are being filtered. Table 2.1 shows the average pore sizes of different membranes used for different applications. On the basis of morphology, membranes can be classified as symmetric, or asymmetric. The symmetric membranes have uniform pore sizes while the pore sizes in asymmetric membranes vary along the radius. It has an inner skin layer that acts as the determining factor for the size of the solute particles that could be filtered and a thick outer layer that provides support to the membranes and aids in mass transfer by adsorption.

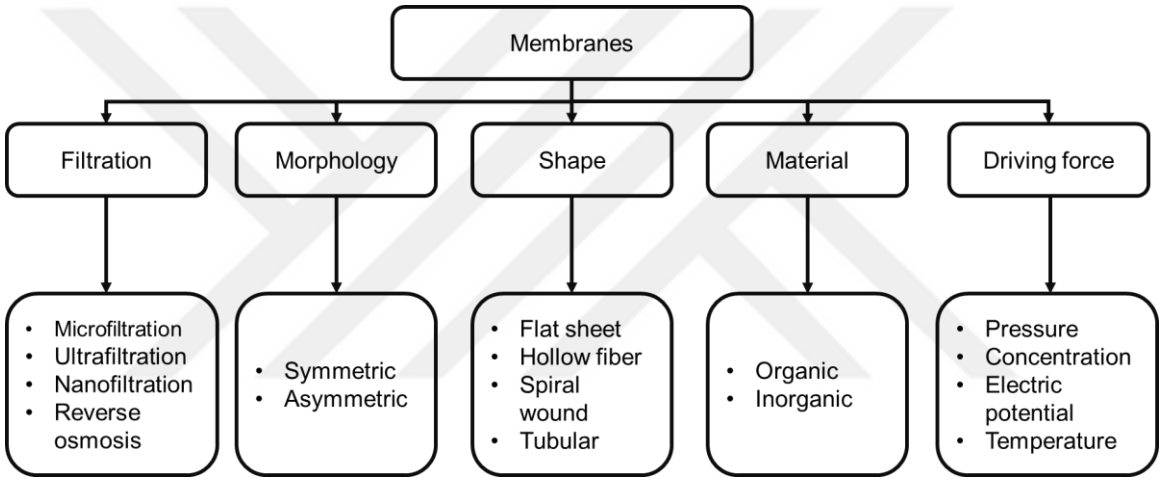


Figure 2.5. Different classification of membranes

Table 2.1 Average pore sizes of different membranes used for different applications adapted from reference [20].

Membrane type	**Average pore size**
Osmosis	0.3 - 0.6 nm
Nano-filtration	≤ 1nm
Ultra-filtration	1 - 50 nm
Microfiltration	50 - 500 nm

Membranes can be classified as flat sheet, hollow fiber, spiral wound, and tubular based on their shape. Hollow fiber membranes are preferable to flat sheet, tubular, or spiral

woven membranes because of their higher surface area per unit volume resulting in higher efficiency. They are also less difficult to produce, and clean, and do not require any mechanical support. Furthermore, each separation process has a driving force that causes the separation of the solute particles. These driving forces can be pressure (positive or negative), concentration, electric potential, and temperature. Hemodialysis is based on the concentration difference between the two sides of the membrane, electrodialysis uses electric potential and membrane distillation uses temperature as the driving force.

Traditionally, hemodialysis membranes have been classified based on their composition as cellulosic (organic) and synthetic membranes. However, due to the presence of hydroxyl groups in the unmodified cellulosic membranes, several cardiovascular diseases as a result of complications like complement, leukocyte, and coagulation activation in contact with blood have caused a massive drop in their usage in the last decade [20]. To overcome the issues (biocompatibility, permeability, etc.) associated with unmodified cellulosic membranes, synthetic membranes were developed more than 40 years ago. The early synthetic membranes due to their thick walls (~100 μm) were not useful with regard to diffusion-based therapies but were rather used only in convection-based therapies (hemofiltration). However, the shortcomings concerning the wall thickness were overcome in the subsequent models. Currently, synthetic membranes have a wall thickness of around 20-50 μm and are effectively being used in high-flux hemodialysis [14].

2.3. Membrane Fabrication Methods

Polymer membranes (both hollow fiber and flat sheet membranes) can be produced using different fabrication methods depending on the polymer type, field of application, type of membrane, average pore size required, etc. These include; Phase inversion, electrospinning, track etching, and sintering.

2.3.1. Phase Inversion

Phase inversion is a process of turning a homogenous polymer solution into two different phases: a polymer-rich phase (matrix) and a polymer-poor phase (pores) [14,20]. Phase inversion can further be categorized into four different types depending on the

desolvation mechanism employed. 1) Non-solvent induced phase separation (NIPS) [22], thermally induced phase separation (TIPS) [23], vapor induced phase separation (VIPS) [24], and solvent-evaporation induced phase separation (SEIPS) [25]. NIPS, TIPS, and VIPS are the most frequently used phase inversion methods, with SEIPS reserved for liquid monomers rather than polymers. Hollow fiber membranes (HFMs) made by phase inversion have distinct physicochemical properties as well as appropriate surface and mechanical properties.

2.3.2. Electrospinning

Advances in the disciplines of nanomaterials and nanotechnologies have aided the emergence of electrospinning as a membrane production process. Electrospinning is a method of producing fibers with diameters ranging from micro to nanometers by using electrostatic forces. To make membranes, electrospinning requires a minimum DC voltage of about 5 kVs [26].

Su, et al. used emulsion electrospinning and sintering to create a new Polytetrafluoroethylene (PTFE) hollow fiber membrane [27]. It's difficult to produce hollow fiber membranes with typical procedures due to PTFE's high solvent resistance and melt viscosity. Pure PTFE nanofiber hollow fiber membranes were first created using an emulsion electrospinning approach with a non-rotating collector, then sintered at high temperatures. As the temperature was increased from 340°C to 3840°C during sintering, the membrane possessed high porosity, superhydrophobicity, and improved mechanical strength. In comparison to commercially made PTFE hollow fiber membranes, the permeate flux increased by 3.2 - 11.6 times.

To make sub-micrometer polyacrylonitrile (PAN) hollow fiber membranes, Anka, et al used a concentric electrospinning approach [28]. The comparatively smooth PAN fibers had average inner and outer diameters of 530 and 890 nm, respectively. The fibers were tested with Indigo carmine dye and NaCl solutions after being inserted into a filtration module. The dye solution passed through the PAN fibers and was replaced by a colorless filtrate, indicating that only water, not dye, passes through the fiber walls. Desalination of the NaCl solution was identical, with a salt rejection of 97.7±0.6 %.

2.3.3. Track Itching

Track etching is a process wherein the polymer is subjected to a heavy-ion beam followed by chemical etching. The chemical bonds present in polymers like polyimide (PI), polyethylene terephthalate (PET), polycarbonate (PC), and PVDF are damaged. This breaking or damaging of the bonds creates nanometer-sized pores. The schematic of a single-ion irradiation setup is shown in Figure 2.6.

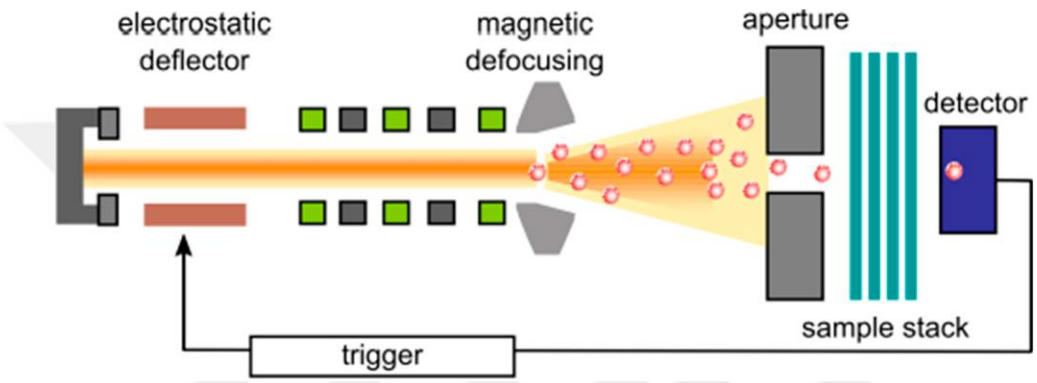


Figure 2.6. A single-ion irradiation setup [29].

The setup consists of an electrostatic deflector, magnetic defocusing instrument, detector, trigger, and sample stack. A tiny circular opening (diameter ~ 200 μm) is utilized to fire single projectiles at a frequency of about 1 Hz once the ion beam has been defocused and calibrated. The ion beam is then used to irradiate a stack of foils. If a solid-state particle detector is put behind the sample, it will register a single ion impact, and an electrostatic chopper device will deflect the entire ion beam.

The ion tracks are then selectively dissolved and expanded into channels in an appropriate etching solution. The pore shape (cylindrical, conical, or cigar-like) and size can be easily controlled during the process (Figure 2.7) [30]. Membranes produced by this process have limited applications like protein adsorption processes.

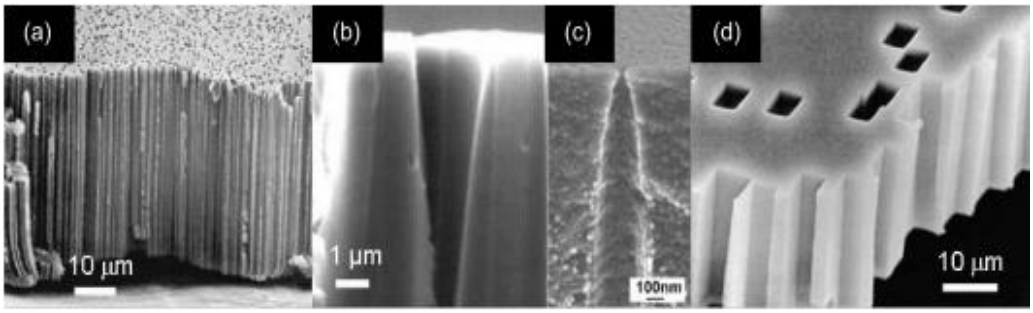


Figure 2.7. Different pore shapes obtained during track itching (a) cylindrical, (b) conical, (c) cigar-like and (d) rhombohedral [30].

2.3.4. Sintering

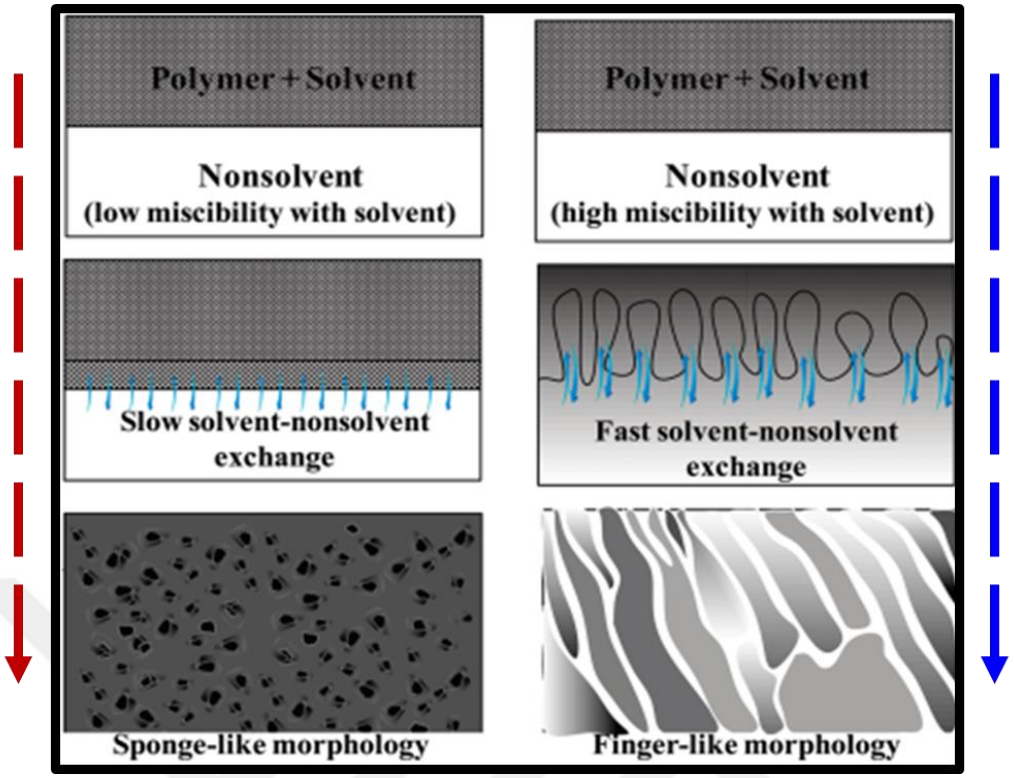
As the name implies, sintering is a high-temperature procedure that involves compacting a specific set of particles to change them into a dense polycrystalline block with great physical and chemical stability. This technique is frequently utilized in the commercial manufacture of inorganic and polymer membranes (polypropylene and symmetric polytetrafluoroethylene). Abdullah et al. used the phase inversion technique to make asymmetric alumina hollow fiber membranes, which were then sintered at high temperatures [31]. To make the ceramic suspension, alumina powder was mixed with polyethersulfone (PES). Polyethylene glycol-30-di polyhydroxy stearate served as a dispersing agent, N-methyl-2-pyrrolidone (NMP) served as a solvent while the ceramic solution served as the polymer binder. The purpose of this work was to examine the self-cleaning characteristics of alumina hollow fiber membranes and the influence of spinning parameters on the creation of asymmetric structures. The findings revealed that finger-like structures could be generated in alumina hollow fiber membranes, with the patterns being controlled by spinning parameters and ceramic suspension. After placing a CuO/CeO_2 catalyst across an alumina membrane support, the catalyst distribution was analyzed using SEM/EDX spectroscopy. Self-cleaning capabilities were studied by comparing them to those of conventional cleaning and UV irradiation for protein rejection. UV self-cleaning increased the permeability to bovine serum albumin (BSA) because of the super-hydrophilicity of the CuO/CeO_2 catalyst.

2.4. Hollow Fiber Membrane Production by Phase Inversion

Commercially, phase inversion is the most well-known and widely used approach for producing membranes. A homogeneous polymer solution is converted into a two-phase system during the process, with a polymer-rich phase forming the matrix and a polymer-poor phase forming the pores [14, 32]. Based on the desolvation mechanism, phase inversion can be of the following four types; non-solvent induced phase separation (NIPS), thermally induced phase separation (TIPS), vapor induced phase separation (VIPS), and solvent-evaporation induced phase separation (SEIPS). NIPS, TIPS, and VIPS are the most commonly used phase inversion methods, while SEIPS is only used in the case of liquid monomers instead of polymers.

The NIPS process involves the preparation of a solution by combining at least a solvent and a polymer (some additives can be mixed with the solution as well, to impart desired properties). This polymer solution is then extruded through a spinneret to generate the desired shape of the membrane. Finally, the extruded polymer is passed through a coagulation bath filled with a non-solvent, and hence, precipitation of the solution takes place due to the exchange of the solvent from the dope solution with the non-solvent coagulation bath (usually water) [33]. Different morphologies of the membranes can be obtained depending on the demixing rate between the solvent and the non-solvent. Instantaneous demixing which corresponds to a high solvent non-solvent miscibility result in a finger-like pore structure while delayed demixing having low solvent non-solvent miscibility produces a sponge-like pore structure and a relatively dense top layer as shown in Figure 2.8 [34].

Even though NIPS is the most widely used membrane fabrication method, TIPS and electrospinning methods are gaining more and more popularity because of their ability to produce membranes with specific characters [35]. Since its introduction in the 1980s, for the production of polyvinylidene fluoride (PVDF), the TIPS method was consequently developed due to the wide adoption of PVDF in micro and ultrafiltration membranes [29]. In the case of TIPS, the polymer solution is prepared at elevated temperatures and cooled to induce phase separation. In this method, a homogenous polymer solution is, demixed by changing the temperature. Upon de-mixing, the formerly homogeneous solution separates into two distinct phases namely; polymer-poor and polymer-rich. This technique is useful for obtaining well-interconnected porous structures [36].



a) b)

Figure 2.8. Membrane morphology based on demixing rates, a) with low miscibility coagulant, and b) with high miscibility coagulant, adopted from reference [34].

Contrary to NIPS, vapor-induced phase separation (VIPS) uses gas as a non-solvent during the phase inversion process. This process is used for the production of flat sheet membranes. The process starts with the preparation of the polymer solution which is cast onto a glass sheet using a casting knife. The cast film is then placed in a controlled relative humidity chamber filled with the non-solvent gas (usually water vapor) for a specific amount of time. After that, the cast is immersed in a coagulation bath (usually water) to solidify the membrane structure [37]. The principal advantage of VIPS-fabricated polymeric membranes is the ability to control morphology with a relatively simple technique. The morphology of the membrane is determined by several factors such as; Solvent and non-solvent composition, polymer concentration, non-solvent vapor exposure time, and relative humidity [29, 38].

2.4.1. Phase Inversion Spinning Processes

There are four types of spinning processes employed for the production of different kinds of polymer fibers: i.e.

1. Dry spinning,
2. Wet spinning,
3. Dry-jet wet spinning and
4. Melt spinning.

2.4.1.1. Dry Spinning

The polymer in dry spinning is initially mixed with a solvent that can easily be evaporated later on after extrusion. This polymer solution is then made to pass through the extrusion machine. The mixture of the polymer and the solution after passing through the spinneret is treated with a stream of hot air or an inert gas that evaporates the mixed solvent leaving a solid filament that can be collected on a take-up wheel Figure 2.9 (a). This spinning process is only used for polymers that cannot be melt-spun because of the safety and environmental concerns associated with solvent handling. Cellulose acetate, cellulose triacetate, Poly (vinyl chloride) (PVC), Polyacrylonitrile (PAN), etc. are some of the common polymers spun with this process [39].

2.4.1.2. Wet Spinning

It is the oldest of all the spinning processes. In wet spinning, the spinneret is submerged in a coagulant bath resulting in the solidification of the jet within the coagulation bath Figure 2.9(b). This method is employed when the solvent cannot be evaporated and must be removed by some other chemical means. This method is more suitable for spinning manmade fibers such as rayon, lyocell, acrylic, etc. [40].

2.4.1.3. Dry-jet Wet Spinning

This method of spinning is an amalgamation of the dry and wet spinning methods. Figure 2.9(c) shows a simple schematic of the dry-wet jet spinning method. The coagulation process began in the air gap region, which contains the most water vapor. The interchange of non-solvent to solvent begins in the air gap zone. The fiber then takes the final form once it enters the coagulation bath. The key element associated with the dry-jet wet spinning technique is the existence of an air gap between the coagulation bath and the tip of the spinneret. This method is used to make fibers with special characteristics. The polymer chains coming out of the coagulation bath have a large degree of orientation along the fiber axis which increases its strength [41].

2.4.1.4. Melt Spinning

This method is used for polymers that can be melted. In this process, the polymer is melted and passed through the spinneret. The solidified fibers are collected on a take-up wheel. The fibers are stretched in both the molten and solidified form. This stretching facilitates the orientation of the polymer chains along the fiber axis Figure 2.9(d). It is the quickest fiber spinning technology currently available. Melt spinning should be used if the polymer is thermoplastic for increased productivity. Melt spinning is used to make the majority of manufactured fibers, such as polyester, polypropylene, nylon, and poly (glycolic acid) (PGA) [42].

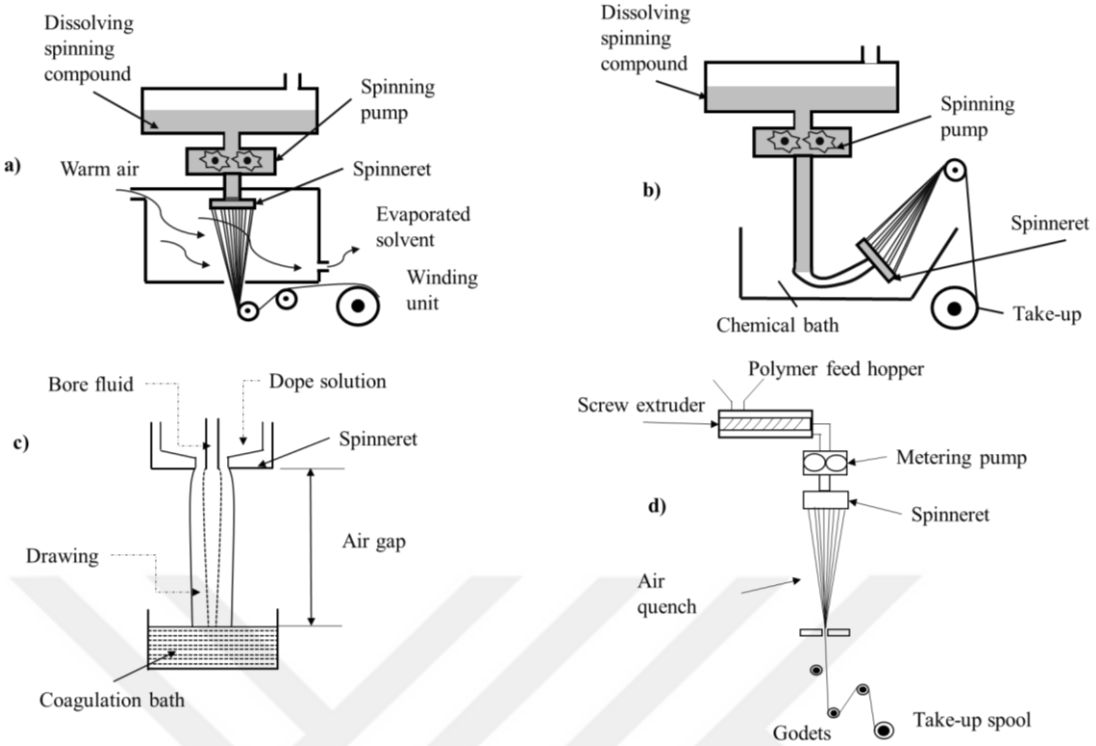


Figure 2.9. Hollow fiber spinning processes. (a) Dry spinning, (b) Wet spinning, (c) Dry jet-wet spinning and (d) Melt spinning; adapted from reference [43].

2.5. Factors Affecting Fiber Characteristics

The characteristic properties and the morphology of hollow fiber membranes are dependent on a variety of factors. By changing the spinning conditions for different membrane materials, innumerable possibilities of membrane properties can be achieved. These factors not only influence the morphological properties like pore shape, size, and distribution but also affects the separation and mechanical properties like permeability, rejection rate, molecular weight cutoff (MWCO), tensile strength, etc. These include polymer type and its concentration, dope extrusion rate, viscosity, solvent and its concentration, additives, bore liquid type and its flow rate, air gap, coagulation bath composition and temperature as well as the take-up speed [44]. Optimization of all the factors while fabricating membranes of required properties is required.

2.5.1. Polymer Type and Concentration

The type of polymer used and its concentration in the process have a huge impact on the outcome of the product. Any kind of separation process requires high chemical and thermal resistance to the fluid being purified. Most commonly used polymers for filtration purposes are Polyethersulfone (PES), polysulfone (PSF), polyvinylidene difluoride (PVDF), polyacrylonitrile (PAN), polyetherimide (PEI), and polyamide (PI).

Bakeri, et al. [45] employed the wet phase inversion method to produce Polyetherimide (PEI) hollow fiber membranes. In the dope solution, the polymer concentration ranged from 10% to 15% by weight. Water was utilized as a coagulant both internally and externally. Membrane characterization was performed by using helium gas permeation tests, liquid entry pressure of water (LEPw) tests, and scanning electron microscopy (SEM). A direct impact of polymer concentration on the morphology of the membranes was observed. As the polymer concentration grew, the average pore size, effective surface porosity, and void percentage of membranes dropped, but LEPw and membrane density increased.

2.5.2. Type of Solvent

The most important factor that determines the choice of a solvent is its miscibility with the polymer. Not all solvents dissolve the exact type of polymers. While studying the effects of solvents like Dimethylacetamide (DMA), Dimethylformamide (DMF), Dimethyl sulfoxide (DMSO), N-Methyl-2-pyrrolidone (NMP), Hexamethylphosphoramide (HMPA), Tetramethylurea (TMU), and Triethly phosphate (TEP), Bottino et al. found that water flux, water content, membrane thickness, and void volume per unit area were influenced by the solvent type [46]. The most commonly used solvents in membrane formation are; dimethylacetamide (DMA), N, N-dimethylformamide (DMF), and 1-methyl-2-pyrrolidine (NMP).

Klein, et al. studied the effects of various spinning parameters on the characteristics of polysulfone hollow fiber membranes [47]. It was observed that PVP of different molecular weights (40,000 and 10,000) affects the hydraulic permeability of the membranes. Higher molecular weight PVP resulted in lower hydraulic permeability and vice versa. This effect was attributed to the increase in the viscosity with the increase in molecular weight.

2.5.3. Type of Additives and Their Concentration

Xu, et al. investigated the effects of PEG molecular weights and concentrations on the filtration properties, morphological structure, and mechanical properties of PES hollow fiber membranes [48]. 25 wt% solids of 20:5:75 (weight ratio) PES/PEG/NMP or 18:7:75 of PES/(PEG600 + PVP40000)/NMP solutions were employed to create asymmetric hollow-fiber membranes using the wet phase-inversion process. The results showed a change in the membrane structure from a double-layer finger-like structure to voids in the shape of spheres or ellipsoids as PEG molecular weights in the dope solution increased from 200 to 10,000; Permeation fluxes of pure water also rose from 22.0 to 64.0 L m^{-2} h^{-1} bar^{-1}. Also, when PVP40000 was included in the dope solution, PES/(PEG600 + PVP40000) hollow-fiber membranes had smoother surfaces (both internally and externally) than PES/PEG hollow-fiber membranes..

2.5.4. Bore Fluid

Bore fluid is one of the most important parameters that dictate the internal morphology of the hollow fiber. The coagulation of the dope begins when it comes in contact with the bore fluid at the end of the spinneret nozzle. Internal precipitation of the solution takes place due to the transfer of the solvent from the dope solution with the non-solvent from the bore fluid [33]. Depending on the demixing rate between the solvent and the non-solvent, different membrane morphologies can be generated. Instantaneous demixing, which corresponds to a high solvent non-solvent miscibility, generates a finger-like pore structure, whereas delayed demixing, which corresponds to a low solvent non-solvent miscibility, produces a porous structure similar to a sponge and a dense top layer [34].

3. RESEARCH METHODOLOGY

3.1. Hollow Fiber Production Setup

The hollow fiber production setup involved the design and construction of three different separate systems.

1. Spinning solution delivery system
2. Bore fluid delivery system
3. Spinneret

3.1.1. Spinning Solution Delivery System

A mechanism similar to an infusion pump was used for this system. It consists of a simple piston-cylinder arrangement (Figure 3.1) mounted on a system of 3D printed parts and a long screw to push or pull the syringe. The direction and speed of the syringe (piston-cylinder arrangement) were controlled by a stepper motor (Nema 23) connected to a controller (Arduino Uno) and push buttons as shown in Figure 3.2. The system was run with a 22V power supply.

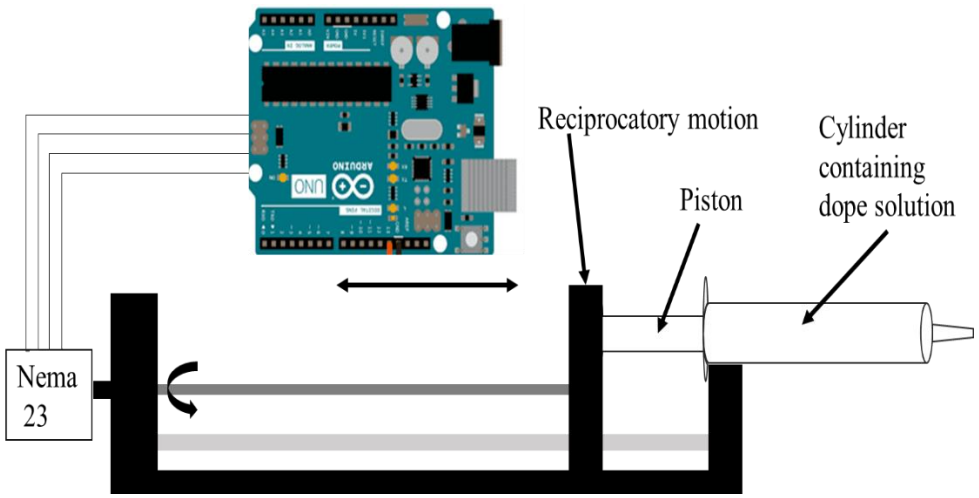


Figure 3.1.Schematic of the spinning solution delivery mechanism established

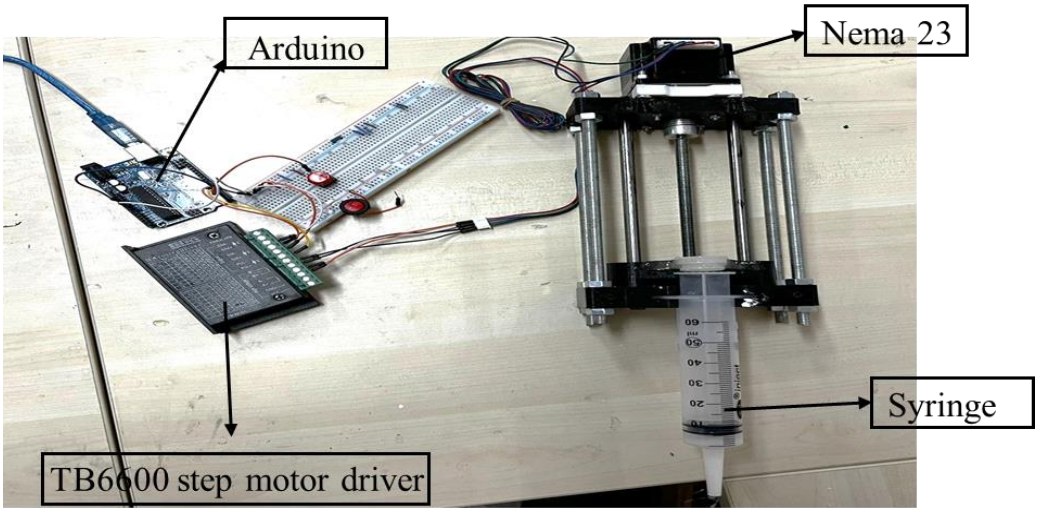


Figure 3.2. Spinning solution delivery system

3.1.2. Bore Fluid Delivery System

It consists of a 5 lt reservoir tank. The bore fluid from this tank was supplied utilizing a small 12V pump. The pump speed and hence bore fluid flow rate was controlled by a 12 V speed controller circuit. A separate 12V power supply was used to power the pump (Figure 3.3).

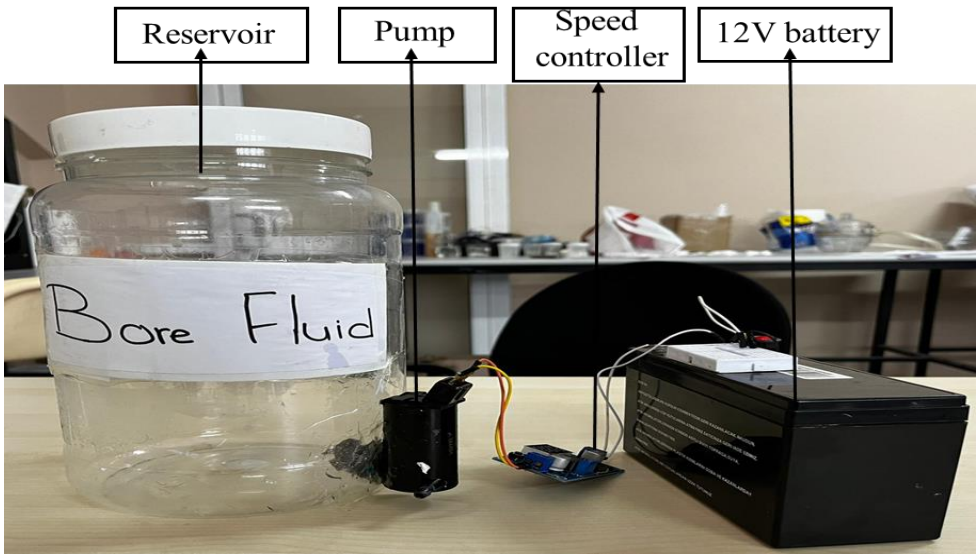


Figure 3.3. Bore fluid delivery system.

3.1.3. Spinneret

A spinneret (Figure 3.4 and Figure 3.5) with two separate inlet and outlet openings for delivering the spinning solution and the bore fluid was designed. The two fluids (dope solution and the bore fluid) meet at the outlet of the spinneret. At this point one can visualize the nascent fiber solidifying as the solvent and non-solvent begin to be exchanged.

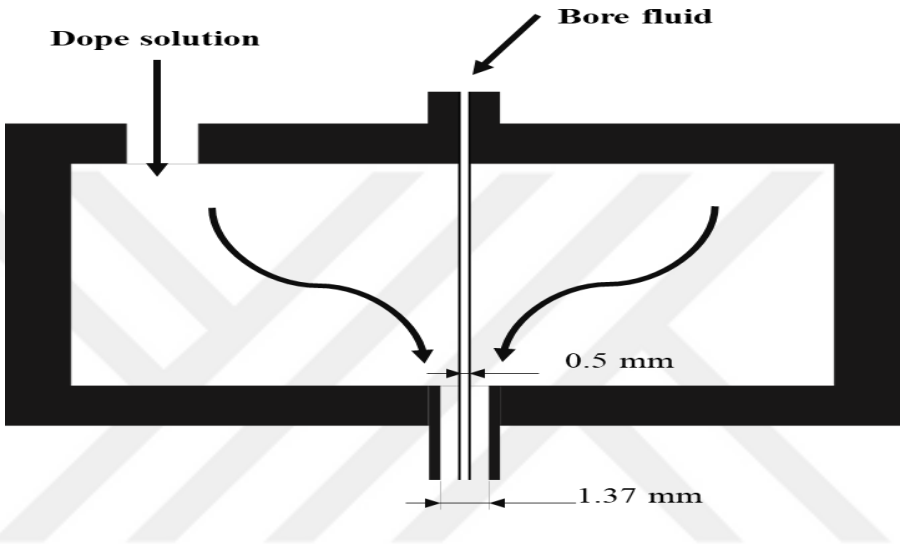


Figure 3.4. Schematic of the designed spinneret

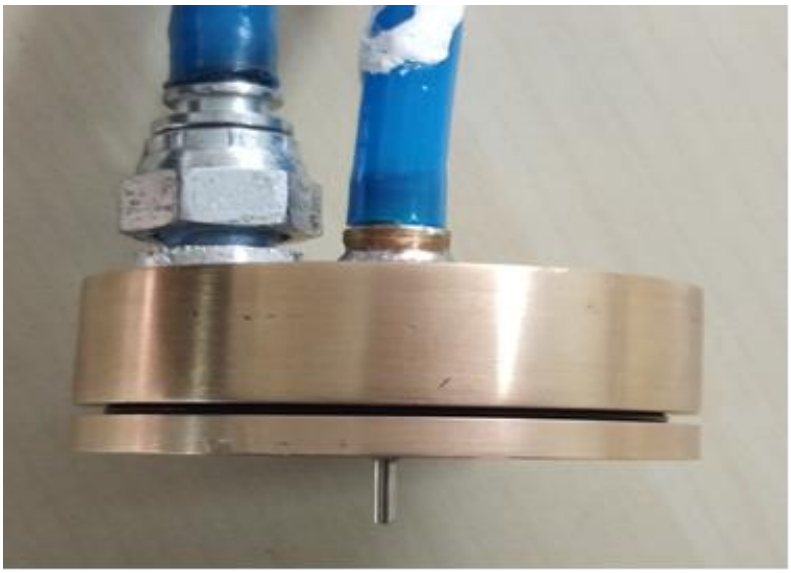


Figure 3.5. Spinneret used in hollow fiber production

3.2. Materials

The current study used BASF Ultrason E 6020P Polyethersulfone (PES) as the membrane-producing polymer matrix. Two different types of pore formers PVP K-30 (Molecular weight of 65,000) and PVP K-90 (Molecular weight of 1,500,000) were used as additives to improve the fiber's viscosity and hydrophilicity (it improves the wettability to prevent protein deposition and adhesion of platelets when exposed to blood). N, N-Dimethylformamide (DMF) was used as the solvent. All the materials for the experiment were provided by BASF Germany. Water and ethanol (96%) are used as bore fluids. Figure 3.6 and 3.7 shows the chemical structure of polyethersulfone and PVP respectively.

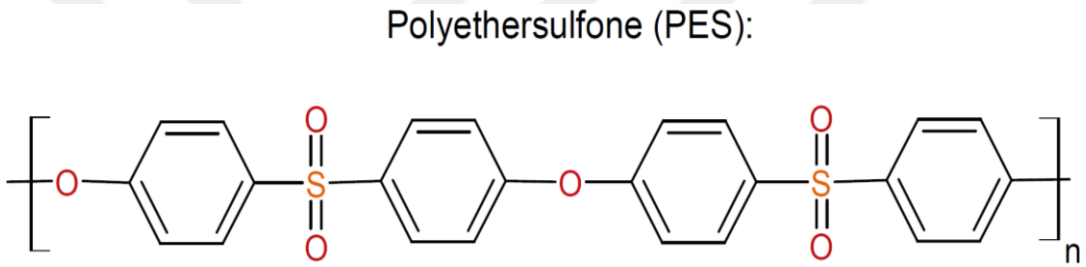


Figure 3.6. Polyethersulfone chemical structure [49].

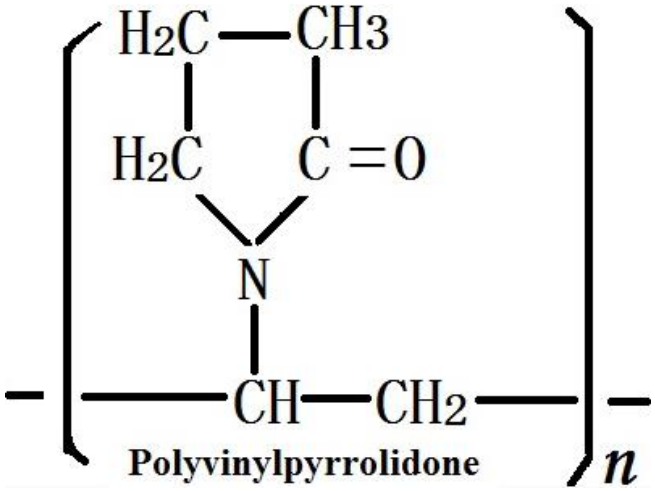


Figure 3.7. PVP chemical structure [50].

3.3. Response Surface Methodology (RSM)

To optimize the production of hollow fiber membranes, response surface methodology (RSM) was used. To create predictive regression models, reduce the number of experiments, and examine the impact of parameters on the response, the Box–Behnken design matrix was used. Preliminary experiments were carried out to screen essential parameters and identify the experimental domain for the production of PES/PVP hollow fiber membranes. Based on the preliminary data and the data from the literature, PES concentration (PES conc.), PVP molecular weight (PVP conc.), bore fluid (BF), and air gap (AG) were chosen as independent variables and labeled as Z_1, Z_2, Z_3, and Z_4, respectively.

The statistical design and data analysis were done with Minitab software. To test the interactions between the primary operating factors and their influences on pure water permeability (PWP) and morphology, the number of tests was optimized using a Box-Behnken design. Table 3.1 shows the operating factor range and variable levels in actual and coded values. Each variable was given a low (-1), middle (0), and high (1) value respectively.

Table 3.1. Box-Behnken design methodology for the experiments

Variable	Factor	Level		
	Z	Low (-1)	Middle (0)	High (+1)
PES conc.%	Z_1	11	14	17
PVP (K30:K90) conc. %	Z_2	0:6	3:3	6:0
Bore fluid (Water: Ethanol) %	Z_3	20:80	60:40	100:0
Air gap (cm)	Z_4	24	37	50

To study four parameters at three levels, the Box–Behnken statistical design requires 27 experimental runs. The central point in the design (PES = 14% wt., K30:K90 = 3:3 % wt., Water: Alcohol = 60:40 % wt, and air gap = 37cm) was repeated three times to determine the errors and the curvature. Table 3.2 shows the experimental plan developed with Minitab.

Table 3.2. Box-Behnken design matrix

Run order	Std. order	PES conc. (% wt.)	PVP conc. (K30:K90) %wt.	BF (Water: Ethanol) %wt.	Air gap (cm)
E1	12	17	3:3	60:40	50
E2	18	17	3:3	20:80	37
E3	4	17	6:0	60:40	37
E4	14	14	6:0	20:80	37
E5	2	17	0:6	60:40	37
E6	26	14	3:3	60:40	37
E7	8	14	3:3	100:0	50
E8	19	11	3:3	100:0	37
E9	21	14	0:6	60:40	24
E10	5	14	3:3	20:80	24
E11	23	14	0:6	60:40	50
E12	24	14	6:0	60:40	50
E13	25	14	3:3	60:40	37
E14	15	14	0:6	100:0	37
E15	20	17	3:3	100:0	37
E16	3	11	6:0	60:40	37
E17	1	11	0:6	60:40	37
E18	9	11	3:3	60:40	24
E19	16	14	6:0	100:0	37
E20	11	11	3:3	60:40	50
E21	6	14	3:3	100:0	24
E22	13	14	0:6	20:80	37
E23	10	17	3:3	60:40	24
E24	17	11	3:3	20:80	37
E25	7	14	3:3	20:80	50
E26	27	14	3:3	60:40	37
E27	22	14	6:0	60:40	24

3.4. Preparation of the Dope Solution

Multiple trial experiments were conducted before choosing the spinning solution concentrations. Experiments with a polymer concentration as high as 25% wt. and an additive concentration of 10% wt. were performed. However, a maximum of 17% wt. of the polymer and 6% wt. of the additives were found to be ideal based on the literature review and the size of the hollow fiber setup.

PES flakes were dried for 3 hours at 80 °C in a furnace before mixing with the solvent. The dope solution was prepared by dissolving PES in DMF at 60 °C. After that, pore formers, PVP K-30, and PVP K-90 were added to the solution. The solution was then mixed using a magnetic stirrer (Figure 3.8) at 600 rpm for at least 12 hours until it became homogenous. The dope solution was then degassed for 2 hours at room temperature in a vacuum chamber (Figure 3.9).



Figure 3.8. Magnetic stirrer used for producing the dope solution

3.5. Hollow Fiber Membrane Fabrication

The dry-wet jet phase inversion method was used to produce the hollow fiber membranes. A schematic of a simple indigenous membrane-producing setup (Figure 3.10) was designed using Nema 23 stepper motor and Arduino. A double orifice spinneret was also indigenously made with inner and outer diameters of 0.50 mm and 1.37 mm. The setup consists of a syringe (piston-cylinder arrangement) controlled by a stepper motor for the dope solution, and a separate reservoir tank attached to a small pump for the bore fluid. Both the fluids are passed through the spinneret through different channels by high-pressure polyurethane hoses.

The fabrication setup is shown in Figure 3.11. It consists of a syringe fitted into an infusion pump mechanism (1). The flow of the dope solution and the bore fluid is controlled by two valves (2) and (5). A bore fluid reservoir (4) is attached to a small pump (6) to pump the bore fluid. The two fluids go through the supply line before converging at the outer tip of the spinneret (3). The nascent fiber after passing through the air gap falls into the coagulation bath (7). Figure 3.12 shows the flow of the nascent fiber coming out of the spinneret.



Figure 3.9. Vacuum chamber to remove residual air bubbles in the dope solution.

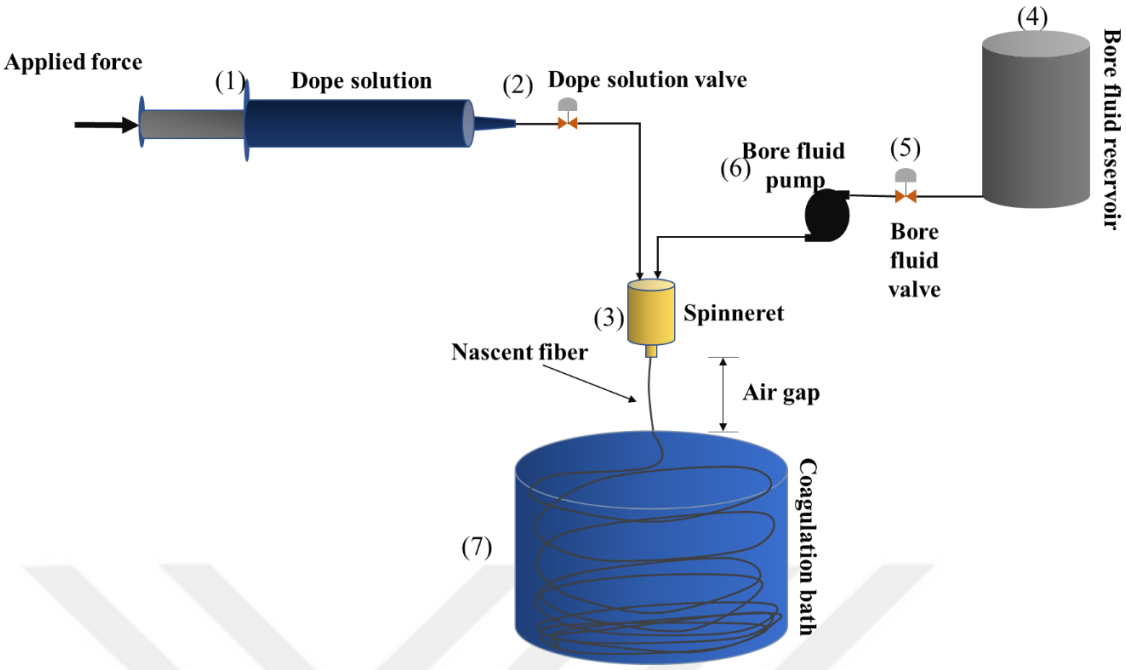


Figure 3.10. Schematics of the hollow fiber production setup

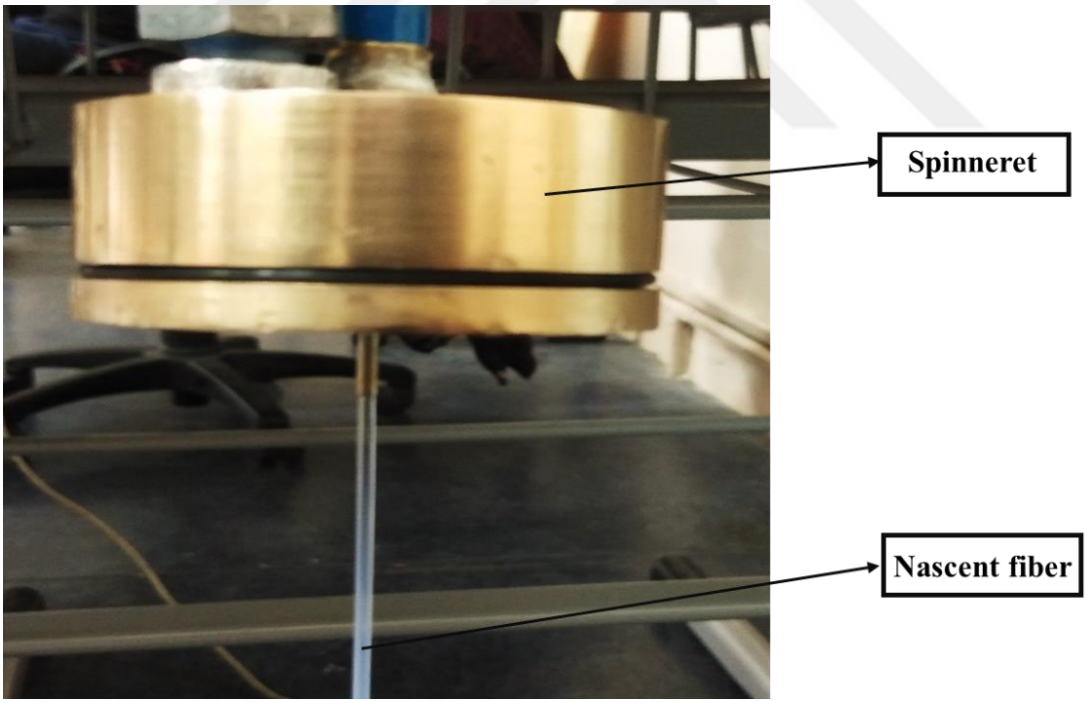


Figure 3.11. Flow of the dope solution through the spinneret



Figure 3.12. Hollow fiber spinning setup.

3.6. Post-treatment of the Fiber

For a single syringe of the dope solution, around 30-40 meters of hollow fiber was produced. The samples were properly categorized and put in a water bath for 12 hours to prevent the pores from collapsing. This also helped in flushing out excess PVP, and residual solvents. After that, the samples were stored in normal water for further testing and analysis (Figure 3.13).



Figure 3.13. Water post-treatment of hollow fiber membranes

3.7. Potting and Module Preparation

Hollow fiber test modules using transparent polyurethane hoses of an inner diameter of 1.1 cm were prepared for the PWP tests. Each module consists of five hollow fibers with effective lengths of 20 cm. Figure 3.14 shows the schematics of the modules. The total length of each module was 28 cm. Two t-fitting connectors were connected at the ends of each module for the inlet and the outlet of the water from the shell sides. The other extreme ends of the t-connectors were connected to small pieces of polyurethane hose pipe which were later sealed using epoxy resin. After that, the potted modules were allowed to air dry for around 12 hours. After the modules were dry, one of the potted ends was cut to allow the flow of the permeate while the other end remained sealed (Figure 3.15).

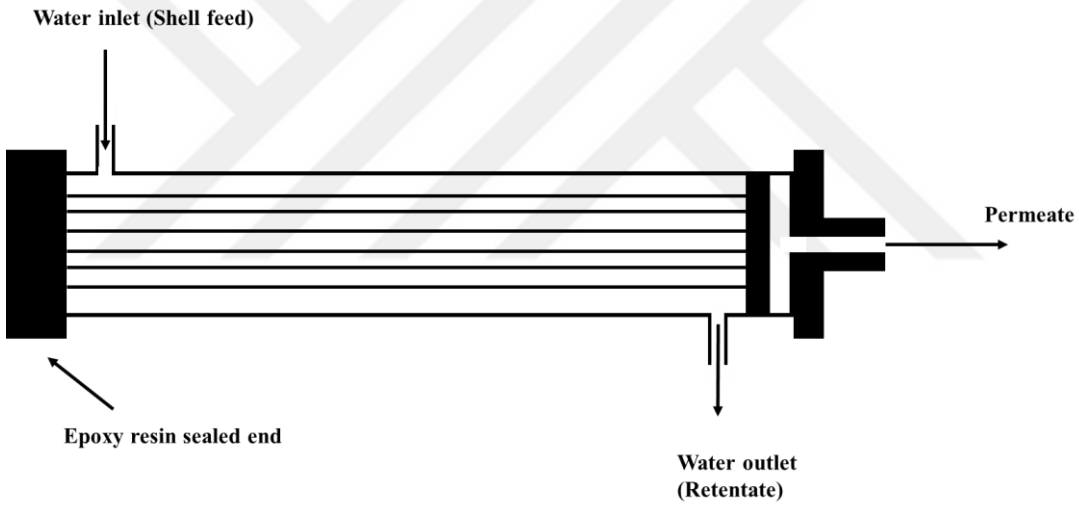


Figure 3.14. Schematics of the potted hollow fiber module

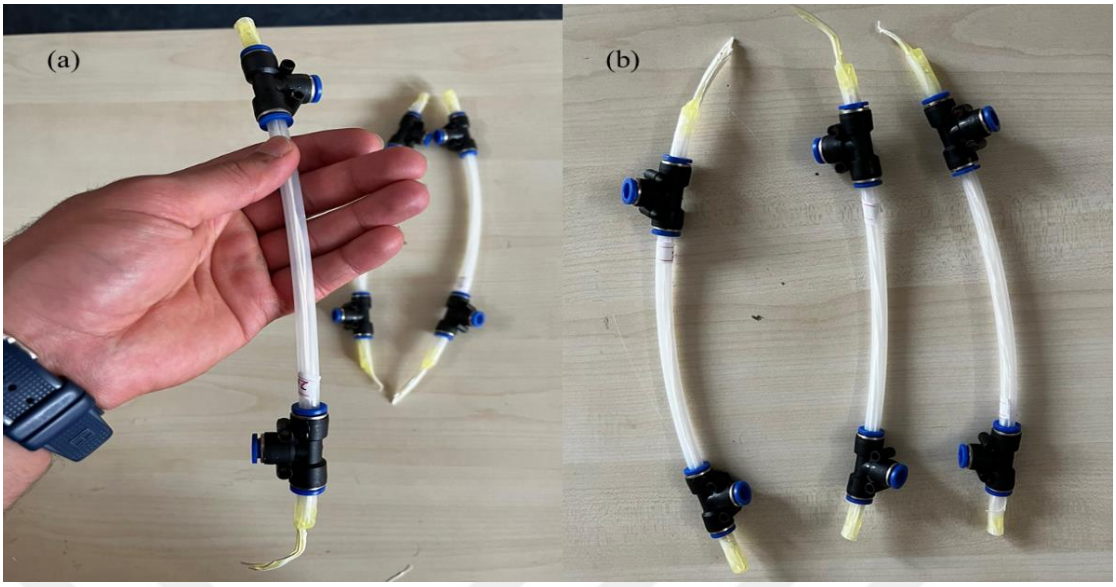


Figure 3.15. Hollow fiber membrane module preparation for pure water permeability tests

3.8. Membrane Characterization

3.8.1. Pure Water Permeability Tests

As can be seen in Figure 3.16, a test setup was constructed to ascertain the PWPof the manufactured membranes. The setup consists of a 1 bar capacity pump, water temperature regulator, flow regulator, pressure gauge, a manometer to measure the transmembrane pressure (TMP) difference, a filter, and a beaker to collect the permeate (Figure 3.16).

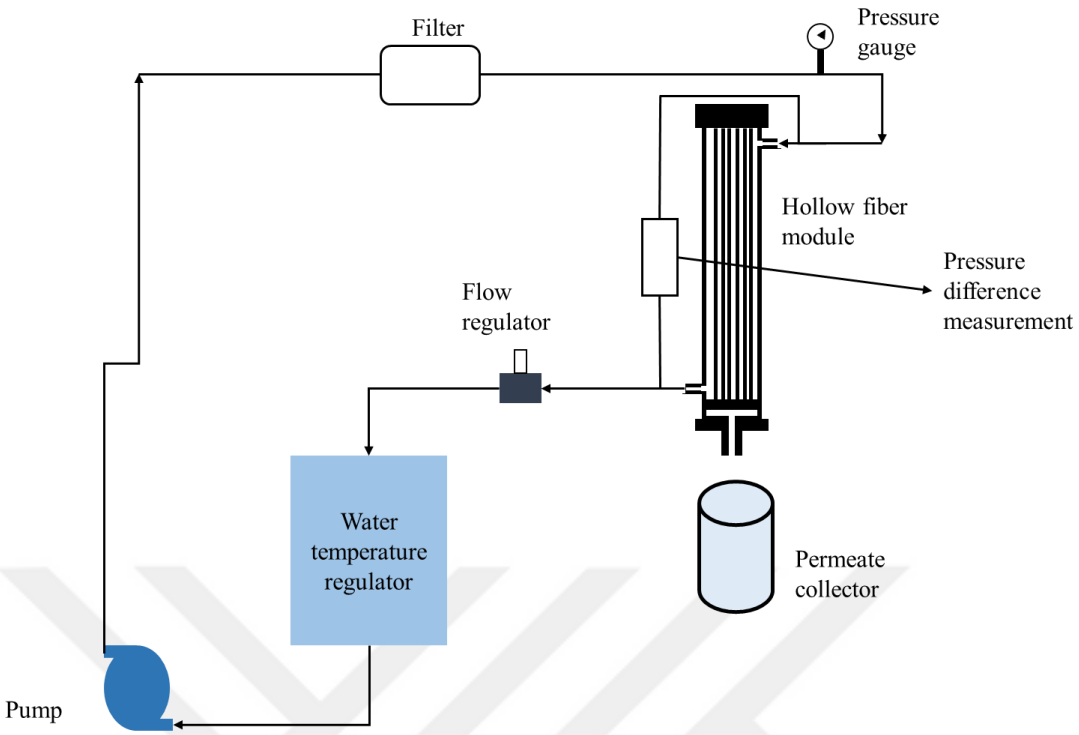


Figure 3.16. Schematics of the hollow fiber PWP test setup

The permeability tests were carried out at a temperature of 25 °C and a feed pressure of 1.0 bar. To measure the PWP, the water from the temperature regulator was pumped through the shell side of the membrane module. The inlet pressure was maintained at 1.0 bar using a flow regulator. Transmembrane pressure (TMP) difference was measured using a digital manometer (Figure 3.16). The modules were pressurized (1 bar) with distilled water for 30 minutes. Using the equation (3.1) below, the amount of permeate that came out of the lumen side was calculated and put into an Excel program [50]:

$$J = \frac{V}{A \times T \times \Delta P} \tag{3.1}$$

Here;

J = Pure water Permeability (L/m^2.h.bar)

V = Volume of permeate (liter)

A = Effective surface area of the membranes (m^2)

T = time (hour)

Figure 3.17 shows the hollow fiber permeability test setup.

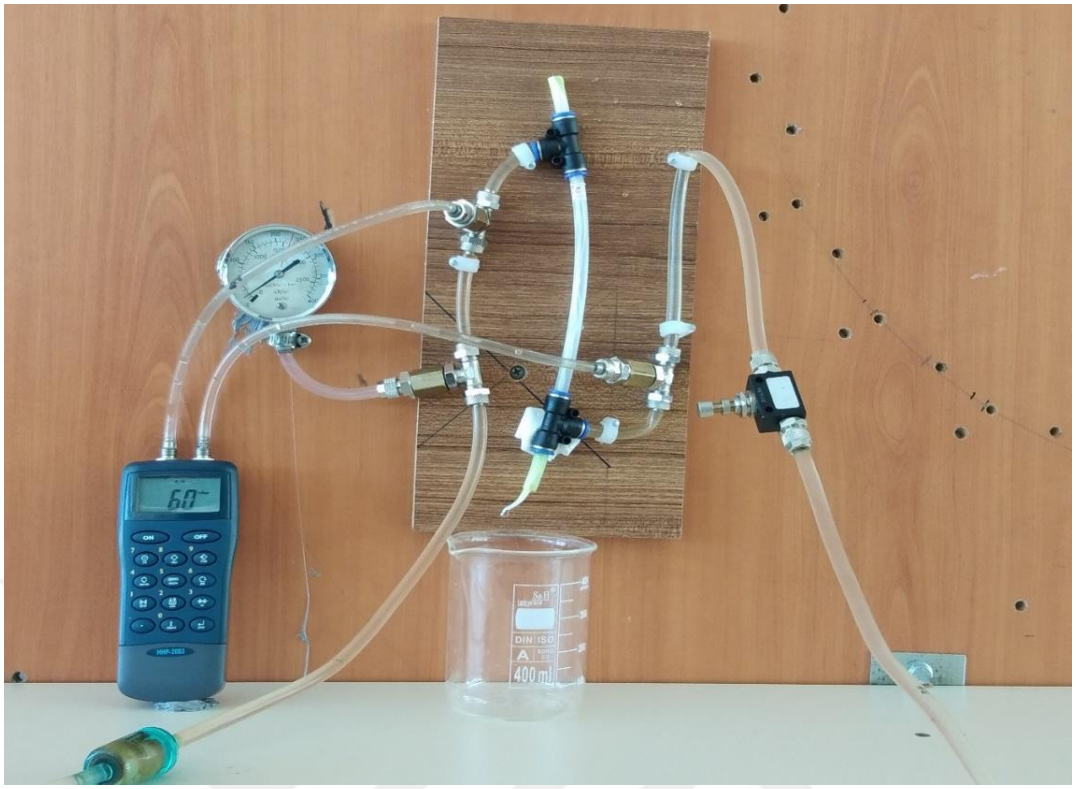


Figure 3.17. PWP test setup

3.8.2. Porosity

The gravimetric porosity of the membranes was evaluated using water. The membrane samples were first dried in an oven for 4-5 hours and then weighed using a precision weighing scale. Then, the membranes were submerged in water for 24 hours and weighed again (Figure 3.18). The resulting values of the weight were put in equation (3.2) to determine the overall porosity of the membranes [52].

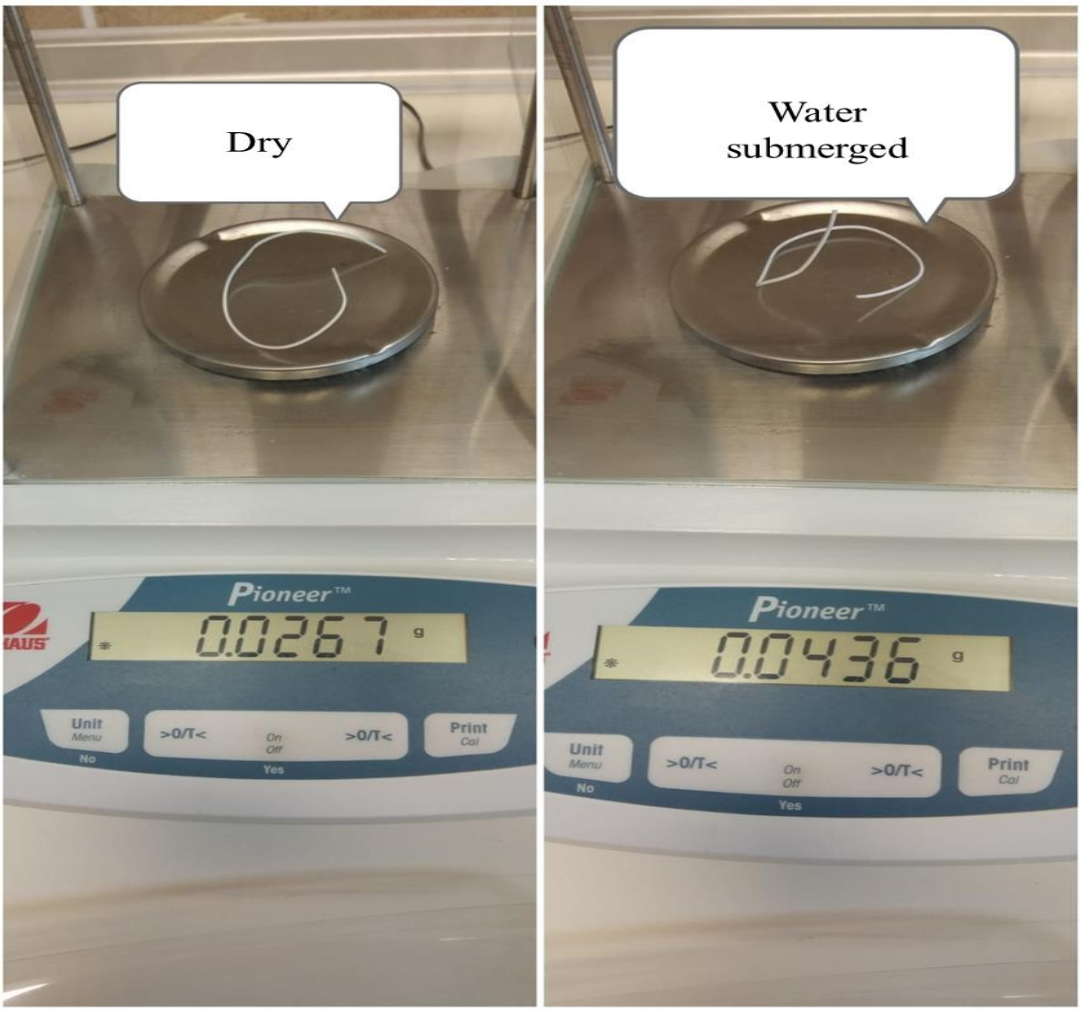


Figure 3.18. Weight of dry and wet membranes using precision a weighing scale

$$\epsilon = \left(\frac{\frac{x_1 - x_2}{\rho_w}}{\frac{x_1 - x_2}{\rho_w} + \frac{x_2}{\rho_p}} \right) \times 100 \qquad (3.2)$$

Here;

ε = Porosity in percentage

x_1 = weight of the wet membrane

x_2 = weight of the dry membrane

ρ_w = density of water (997 kg/m^3)

ρ_p = density of the polymer (1370 kg/m^3)

3.8.3. Scanning Electron Microscopy (SEM) Analysis

The morphology of the fabricated samples was analyzed using ZEISS EVO scanning electron microscope (Figure 3.19). Prior to the test, the samples were prepared by submerging them into liquid nitrogen for a few seconds and then carefully fracturing them. Before mounting the samples into the SEM, they were arranged in a line on a mount (Figure 3.20). Samples were then gold-sputtered using an SPI sputter coater (Figure 3.21) with a 5-10 nm thick layer of gold for a few minutes to induce electrical conductivity.



Figure 3.19. ZEISS EVO scanning electron microscope (SEM).

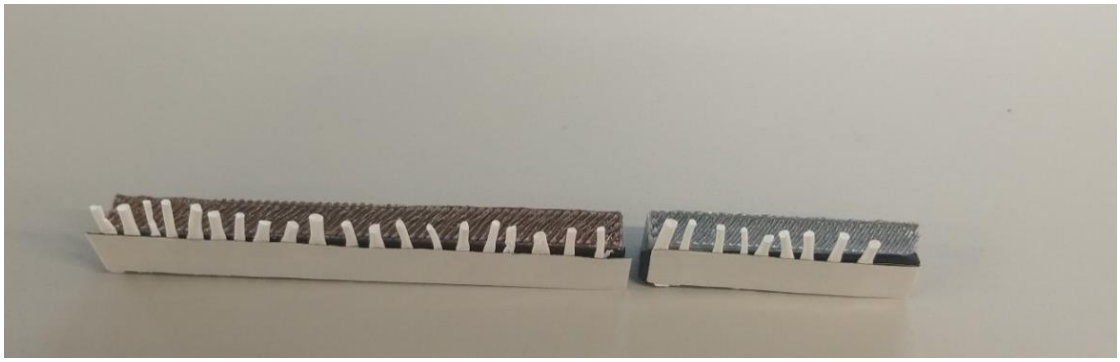


Figure 3.20. Samples attached on the sample mount



Figure 3.21. SPI gold sputter coater used to coat membrane samples for SEM analysis

3.8.4. Pore Size Distribution

The pore size distribution of the membrane with asymmetric morphology was evaluated using ImageJ software. Then, a comparison of the pore size distribution of sample E5 (asymmetric morphology with the lowest pure water permeability) and sample E16 (columnar intrusion cellular with the highest pure water permeability) was performed.

4. RESULTS AND DISCUSSIONS

4.1. Determining The Spinning Solution Concentration Range

Before choosing an appropriate range for the spinning solution, multiple trials with a variety of polymer, additives, and solvent concentrations were conducted. Some spinning parameters were modified with each trail, including polymer concentration, additives concentration, solution flow rate, bore fluid flow rate, air gap, etc. Multiple problems like too high viscosity for the machine setup, too low viscosity for smooth laminar flow, rough surfaces, high solution flow rate, etc. were encountered. A polymer concentration range of 11-17% and a PVP concentration of 6% were found to be ideal for optimum results. This range was also feasible with the capacity of the setup. Table 4.1 shows the recipes used during the trials.

Table 4.1. Trial recipes used for optimization

Trial number	**Compositions**						
	Spinning solution				**Bore fluid**		
	PES (%wt.)	**PVP (K:30 %wt.)**	**PVP (K:90 %wt.)**	**Solvent (DMF % wt.)**	**Water (% wt.)**	**Alcohol (% wt.)**	**Air (%wt.)**
1	25	5	-	70	100	-	-
2	25	-	5	70	100	-	-
3	25	2.5	2.5	70	100	-	-
4	20	2.5	2.5	75	100	-	-
5	20	2.5	2.5	75	-	-	100
6	15	5	-	80	100	-	-
7	15	-	5	80	50	50	-
8	15	2.5	2.5	80	50	50	-
9	15	2.5	2.5	80	-	100	-
10	15	2.5	2.5	80	-	-	100
11	12	3	3	82	100	-	-
12	12	6	-	82	100	-	-

Table 4.1. Continued

13	12	-	6	82	100	-	-
14	12	3	3	82	50	50	-

4.2. Spinning Conditions

Spinning conditions significantly affect the final quality of the membrane. To get optimum results, the spinning process should be conducted in a controlled environment. There are many factors affecting the properties of hollow fiber membranes. During this study, the effects of only four parameters (PES conc., PVP conc., bore fluid composition, and air gap) was thoroughly studied. Other parameters like dope solution flow rate, bore fluid flow rate, bore fluid temperature, coagulation bath temperature, and take-up speed were kept constant. Table 4.2 shows the list of those parameters and their values.

Table 4.2. Values of the controlled parameter

Parameter	Value
Spinning solution flow rate (ml/min)	8
Bore fluid flow rate (ml/min)	24
Bore fluid temperature (◦C)	25
Coagulation bath	Water
Coagulation bath temperature (◦C)	25
Take-up speed	N/A

4.3. Results of SEM, PWP and Porosity

Figure 4.1 shows the SEM images of the cross-sections of all 27 samples in sequential order. Prior to the SEM test, all the samples were carefully prepared. To reveal clean cross sections of the membranes, the samples were initially dipped into water for 10 seconds and then submerged into liquid nitrogen for a few seconds, and then fractured carefully. This process enables a clean cut of the membrane without distorting its porous structure.

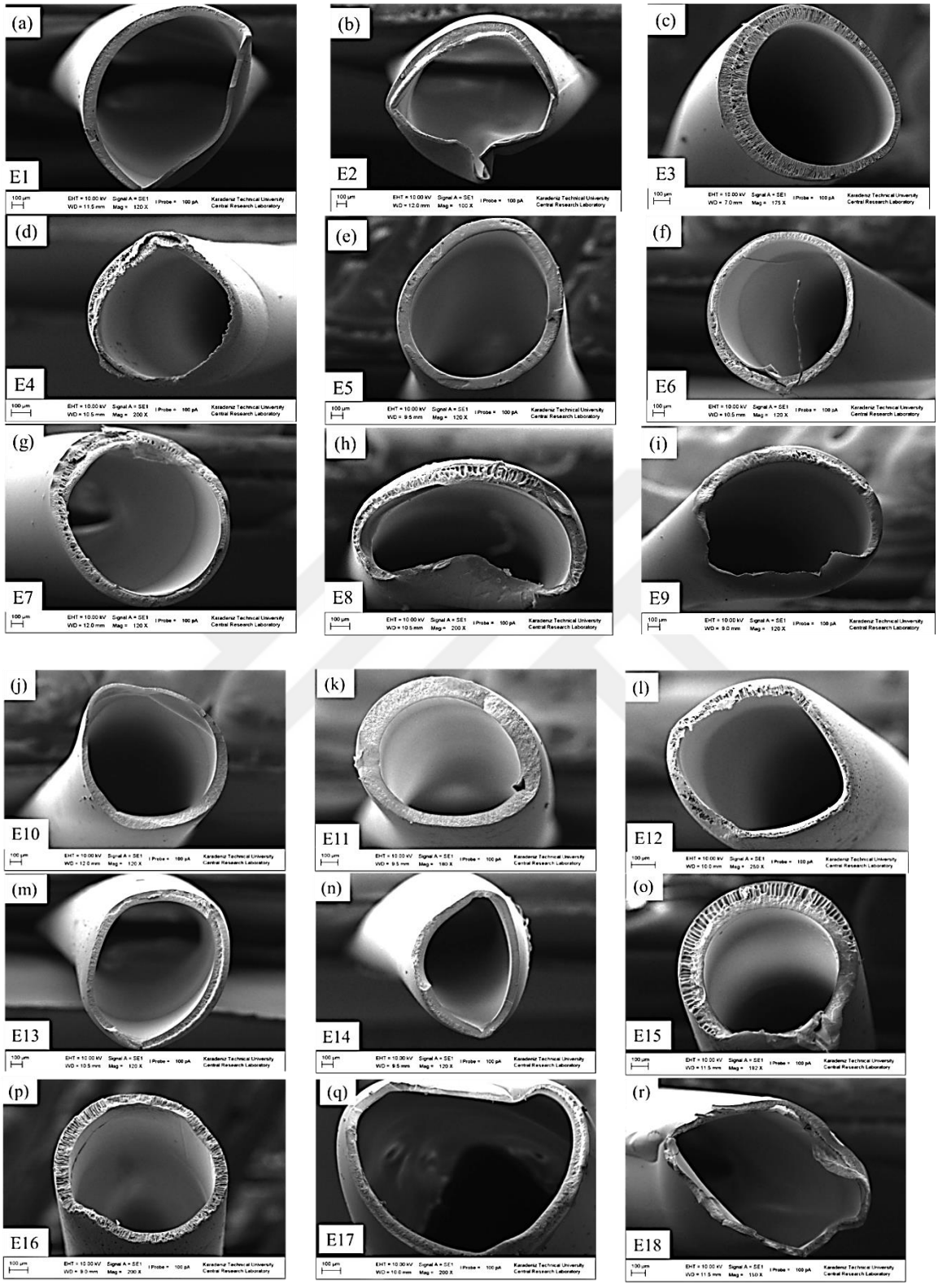
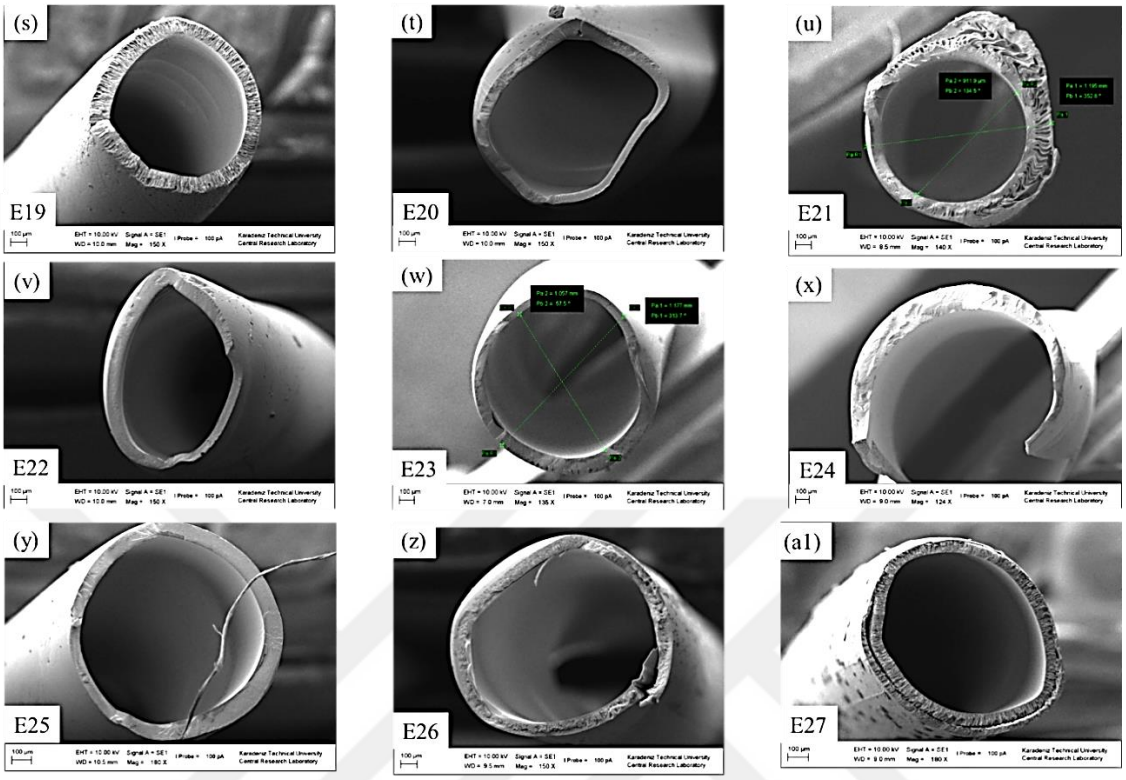


Figure 4.1. Images of the 27 membrane samples taken with a scanning electron microscope

Figure 4.1. Continued



From Figure 4.1, it can be observed that different morphological structures of the membranes with varying spinning conditions were obtained. Some fibers have macro voids and intrusion cells. However, fibers with spongy structures (both symmetric and non-symmetric) were found as well. Table 4.3 shows the results of the PWP and porosity of the membrane samples.

Table 4.3. PWP test and porosity measurement results.

Run order	Std. order	PES conc. (wt%)	PVP conc. (K30) %	BF (% of water)	Air gap (cm)	Wall thickness (µm)	PWP ($l/m^2.h.bar$)	Porosity (%)
E1	12	17	3	60	50	61	98,10	48,12
E2	18	17	3	20	37	82.5	44,97	46,63
E3	4	17	6	60	37	102.2	103,21	48,56
E4	14	14	6	20	37	56.5	151,38	49,55
E5	2	17	0	60	37	102.5	24,78	51,64
E6	26	14	3	60	37	79	105,60	56,43
E7	8	14	3	100	50	110.5	212,09	61,14
E8	19	11	3	100	37	165	252,08	66,83

Table 4.4. Continued

E9	21	14	0	60	24	84	79,05	60,79
E10	5	14	3	20	24	89.5	75,50	53,17
E11	23	14	0	60	50	125.5	82,53	56,89
E12	24	14	6	60	50	428.5	203,40	52,83
E13	25	14	3	60	37	93	129,81	55,77
E14	15	14	0	100	37	89.7	105,87	61,25
E15	20	17	3	100	37	60	85,50	50,19
E16	3	11	6	60	37	69	452,22	70,82
E17	1	11	0	60	37	72	101,91	72,15
E18	9	11	3	60	24	64	171,55	65,37
E19	16	14	6	100	37	104.6	302,47	56,17
E20	11	11	3	60	50	77.2	228,56	62,33
E21	6	14	3	100	24	141.5	154,4	59,83
E22	13	14	0	20	37	72.3	67,78	59,88
E23	10	17	3	60	24	59.8	72,99	49,66
E24	17	11	3	20	37	87	140,03	60,37
E25	7	14	3	20	50	60	97,70	51,73
E26	27	14	3	60	37	104.5	118,78	58,59
E27	22	14	6	60	24	77.2	169,24	54,11

4.4. Effect of Various Parameters on The Morphology of Membranes

4.4.1. Effect of Polymer Concentration on Morphology

Three different polymer concentrations of 11%, 14%, and 17% were investigated. SEM imaging of the membranes showed a decrease in the pore size with the increase in the polymer concentration (Figure 4.2).

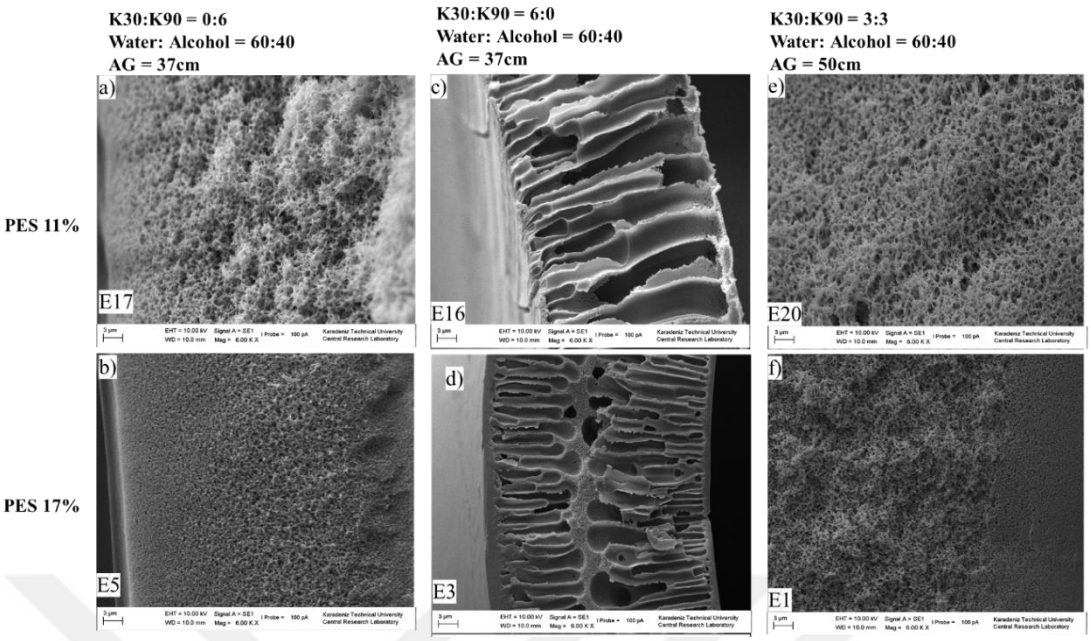


Figure 4.2 Variation of pore size with polymer concentration.

The concentration of the polymer has a direct impact on the system's viscosity. Thus, the higher the concentration of the polymer, the higher the resistance to the diffusion of the non-solvent (water and alcohol in this case) into the polymer-rich phase resulting in finer pores. From Figures 4.2 a) and b), it can be observed that, as the polymer concentration is increased from 11% to 17% while keeping all the other spinning parameters constant (K30:K90 = 0:6, water: alcohol= 60:40, and AG = 37 cm), the pore sizes of the resulting polymer are refined. The same can be observed in Figures 4.2 c), d) and e), f).

Liu et al. studied the effect of the PES dope concentration on the morphological properties of PES/PDMS HF membranes [53]. They found that an increase in the polymer concentration results in a decrease in the mean pore size as well as the gas permeance. Similar results were found by R. Naim, and A.F. Ismail while studying the effect of polyetherimide (PEI) concentration on the morphology and performance characteristics of PEI hollow fiber membranes [54].

4.4.2. Effect of Additives on Morphology

Additives or pore formers are important to introduce desired properties into a membrane. Properties like hydrophilicity, permeability, rejection rate, and molecular weight

cut-off (MWCO) can be fine-tuned by the use of additives. Two different types of PVP additives, K30 and K90 with molecular weights of 44,000 g/mol and 1,100,000 g/mol were used for the experiments. The overall additive concentration in the solution was kept constant at 6%. The results showed that the use of a lower molecular weight additive (K30) produced intrusion cells. While the use of higher molecular weight PVP yielded spongy structures (Figure 4.3).

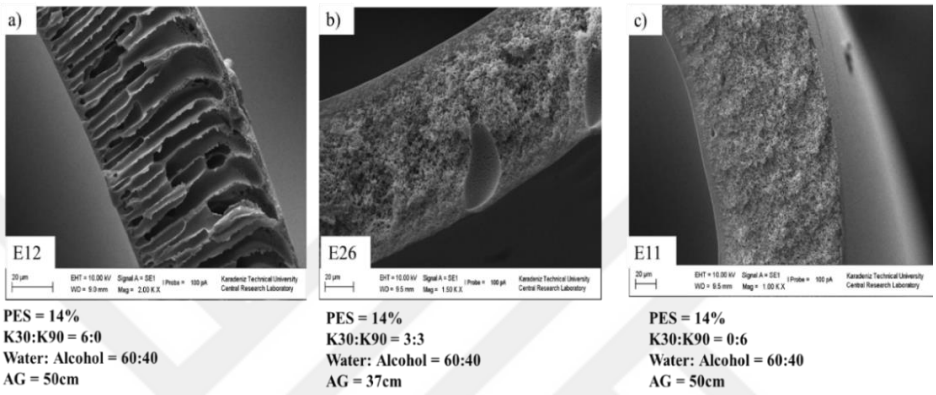


Figure 4.3 Effect of additive molecular weight on PES morphology.

As seen in Figure 4.3, when the ratio of K30:K90 changes from 6:0 (Fig. 4.3(a)) to 3:3 (Fig. 4.3(b)) and finally to 0:6 (Fig. 4.3(c)), the membrane morphologies changes from intrusion cells to macro voids to spongy structure respectively. This can partly be attributed to the increase in the viscosity of the spinning solution due to the higher molecular weight of the K90 additive.

Studies by Xu et al, on the effects of PVP molecular weights on the separation properties as well as the morphology of PEI hollow fiber membranes, showed similar results [55]. They used PVP of different molecular weights (10,000, 40,000, and 130,000 g/mol). The results of the study showed with increasing PVP molecular weights, the morphology of the membranes changes from finger-like intrusion cells to spongy structures.

4.4.3. Effect of Bore Fluid on Morphology

The quenching medium (bore fluid) composition has a huge impact on the morphology of a membrane. The quenching power or the miscibility of the precipitants facing the membrane surfaces determines the intensity and the location of the intrusion cells and

cavities. The general conclusion, which is consistent with existing literature, is that low concentration solutions, when paired with a moderately potent precipitant, enhance the formation of intrusion cells and cavities.

During the current study, a combination of water and alcohol was used as bore fluid. Six out of the 27 samples were prepared with water as the bore fluid. Figure 4.6 shows the morphology of those six samples.

Five out of six samples (Figures 4.4 a), b), d), e), and f)) exhibited the presence of finger-like intrusion cells and macro voids. This characteristic behavior can be ascribed to the high quenching power or miscibility of the water. Figure 4.4 c), even though water quenched as well, exhibited asymmetric spongy structure. Unlike the other five samples, sample E14 (Figure 4.4 c)) had a 6% of high molecular weight PVP (K90) concentration.

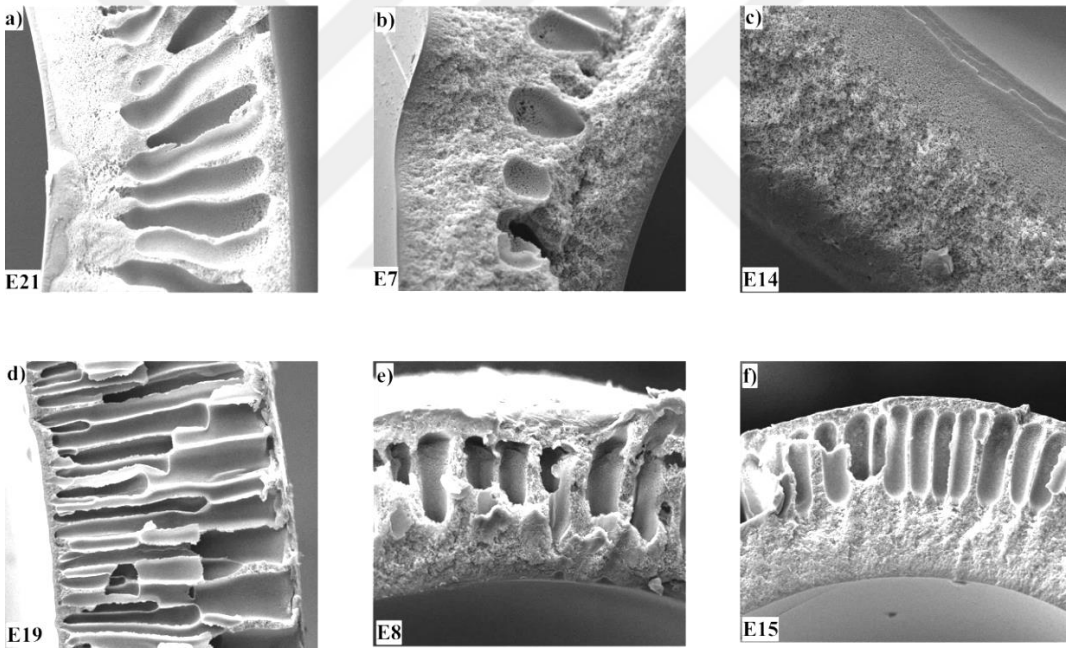
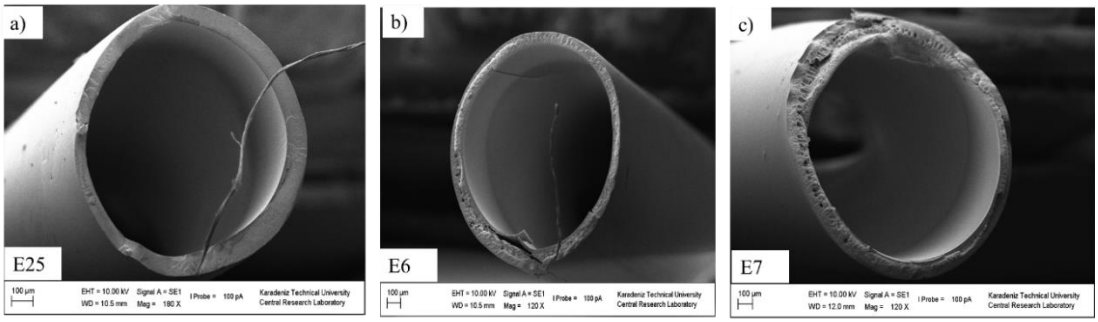


Figure 4.4 Effect of water on the morphology of PES membranes.



PES = 14%
K30:K90 = 3:3
Water: Alcohol = 20:80
AG = 50cm

PES = 14%
K30:K90 = 3:3
Water: Alcohol = 60:40
AG = 37cm

PES = 14%
K30:K90 = 3:3
Water: Alcohol = 100:0
AG = 50cm

Figure 4.5 Change in morphology with variation in bore fluid.

The implications of varying the bore fluid's water-to-alcohol ratio are depicted in Figure 4.5. Lower concentrations of water (water: alcohol = 20:80) produced spongy structures. However, increasing the water content or lowering the alcohol content gave rise to macro voids and intrusion cells.

Otitoju, et al, studied the effect of ethanol on the properties and morphology of PES hollow fiber membranes [56]. The study found an inverse relationship between the alcohol concentration and the pore sizes. The pore sizes increased with a reduction in alcohol concentration.

4.4.4. Effect of Air Gap on Morphology

Air gap has been demonstrated to directly alter the membrane wall thickness and the skin layer thickness in studies of the effects of air gap on the properties of hollow fiber membranes. Ahmad *et al* while working on the effects of air gap on the PES/ PVA hollow fiber membranes found that the increase in air gap from 5 cm to 20 cm reduced the outer diameter size from 0.881mm to 0.724 mm, while the inner diameter changed from 0.564 mm to 0.464 mm respectively [57].

As far as the current study is concerned, the range of the air gap was kept between 24 cm to 50 cm. A variation in both the wall thickness and the inner skin layer thickness was observed with an increasing air gap. Figure 4.6 shows the effect of the air gap on the wall thickness and the inner skin layer thickness.

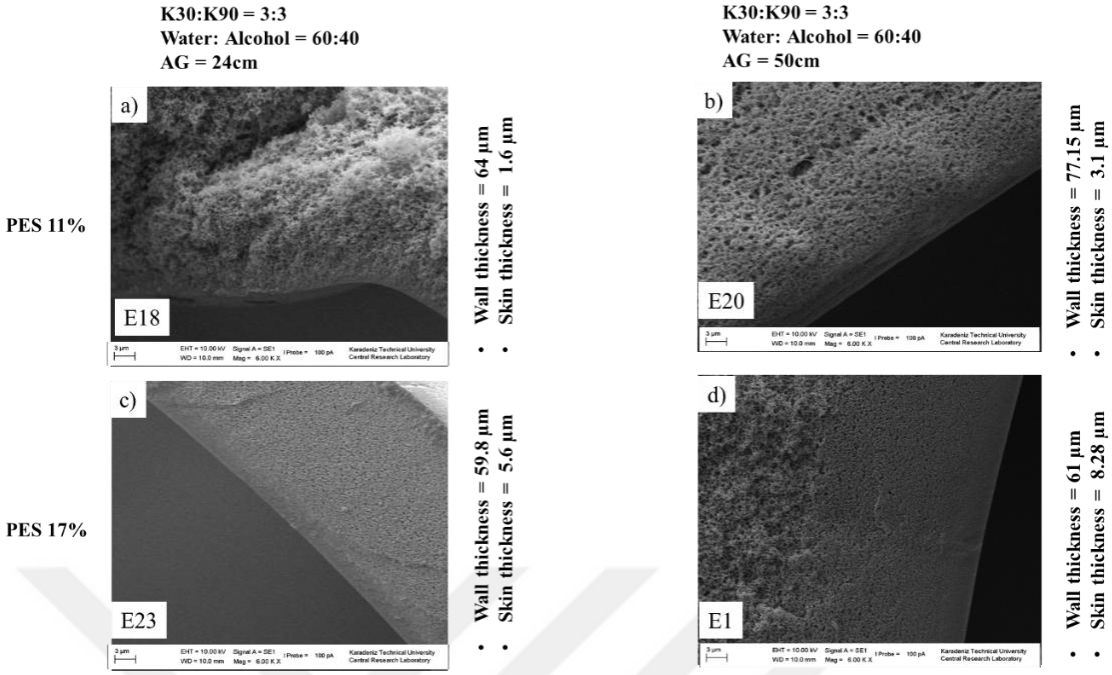


Figure 4.6 Variation of wall thickness and inner skin layer with the air gap.

From the figure, it can be observed that the wall thickness and inner skin layer thickness increased with an increasing air gap. For example, at 11% PES concentration, the membrane's wall thickness rose from 64 µm to 77.15 µm, while the inner skin layer thickness increased from 1.6 µm to 3.1 µm respectively. Similarly, at 17% PES concentration, the wall thicknesses increased from 59.8 µm to 61µm and the corresponding inner skin layer thickness increased from 5.6 µm to 8.3 µm respectively. One thing to be noted here is that there is not much increase in the wall thickness for 17% PES concentration. This is attributed to the higher PES concentration (resulting in higher viscosity) leading to less expansion of the nascent fiber.

4.5. Effect of Various Parameters on Pure Water Permeability

The PWP is mostly reliant on the membrane's hydrophilicity and permeability. The effects of various spinning parameters on PWP have been extensively studied by various researchers. Bakeri et al, studied the effects of polymer concentration on the performance and morphology of PEI membranes using the wet phase inversion method [58]. The PEI content in the solution varied from 10-15%, and water quenched both internally and

externally. The average pore size, porosity, and void fraction showed a decrease with an increase in polymer content.

Alsalhy *et. al* produced PES hollow fiber membranes using gamma butyrolactone (GBL) and polyethylene glycols (PEGs) as the solvent and the additives respectively [52]. Pure water and 30wt% each of ethanol and isopropanol were utilized as bore fluids. The effects on permeability, separation performance and mechanical properties of the polymer due to PEG concentration, bore fluid type, and bore fluid flow rate were examined. By increasing the bore fluid flow rate from 7.67 to 23.06 g/min, the PWP was seen to rise from 45.2 to 107.4 l/m^2. h. bar.

The effects of PVP on the polysulfone membranes was studies by Eren *et al*. It was found that increasing the PVP concentration changes the morphology of the macroviods (both shape and size). Also increasing the PVP concentration from 0 to 10 wt% resulted in a change in pure water flux (PWF) from 36.76 to 86.80 l/m^2h [59].

The results from the study on the effects of pore formers on the production of poly (vinylidene fluoride-co-hexafluoropropylene) (PVDF-HFP) HF membranes by Lei Shi et al, showed an increase in the permeability of the hollow fiber membranes as the glycerol (additive) concentration was increased from 2% to 10%. These results are in line with the results obtained from the current study [60]. Since PES is hydrophobic, an increase in the concentration of the hydrophilic PVP results in an increase in PWP. The results in Table 4.3 show a decrease in the PWP as the concentration of the polymer is increased while it increases with an increase in additive concentration. The lowest permeability found was 24.781 L/m^2.h.bar at 17% polymer concentration while the highest permeability value found was 452.225 l/m^2.h.bar at 11% polymer concentration.

Figures 4.7 a) to g) and Figure 4.8 a) to g) show the variation of the PWP as 3-dimensional response surface plots and contour plots with varying input parameters.

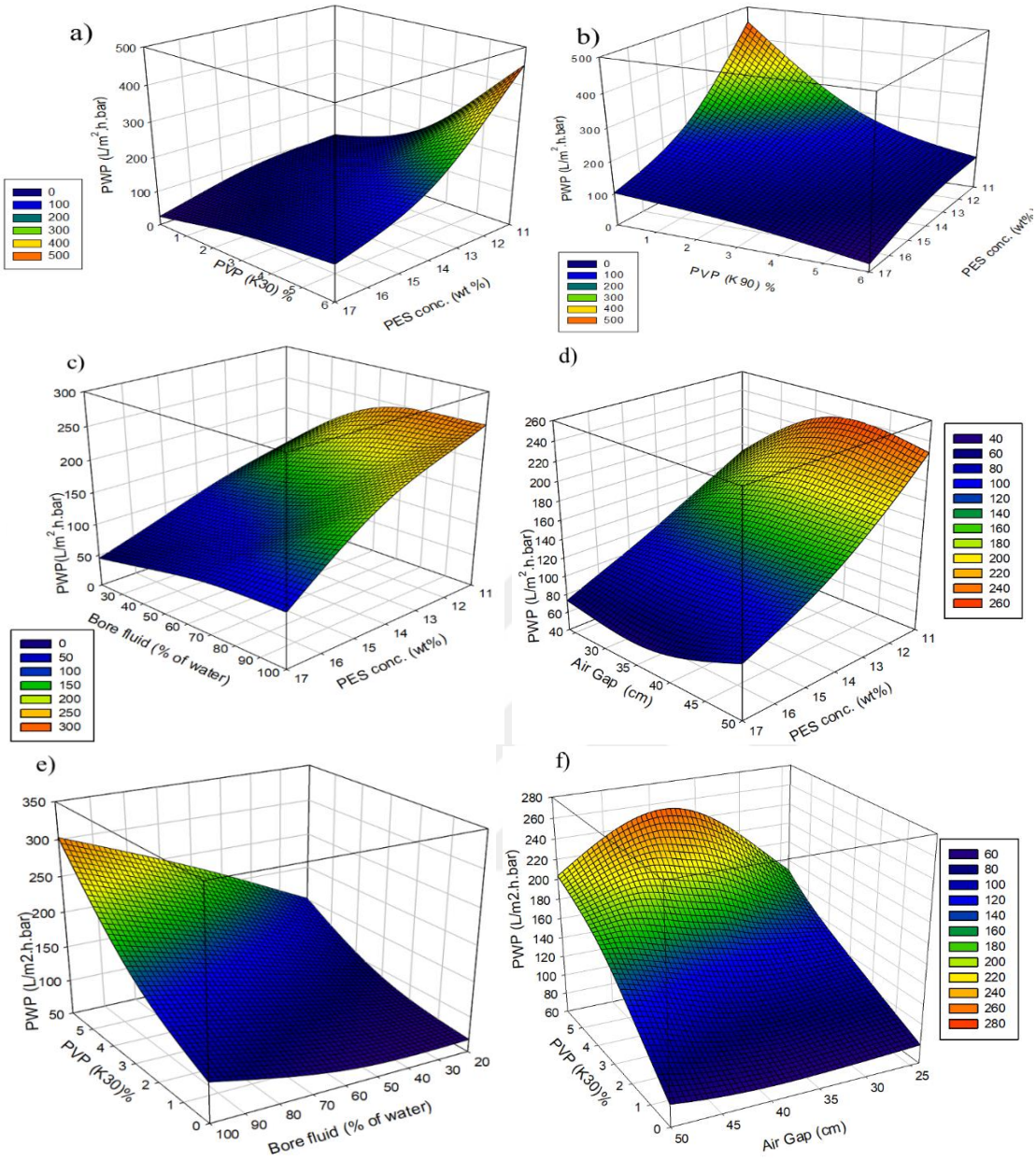


Figure 4.7. 3-dimensional response surface plot for pure water permeability in response to (a) polymer concentration and PVP (K30), (b) polymer concentration and PVP (K90), (c) polymer concentration. and bore fluid and (d) polymer concentration and air gap, e

Figure 4.7. Continued

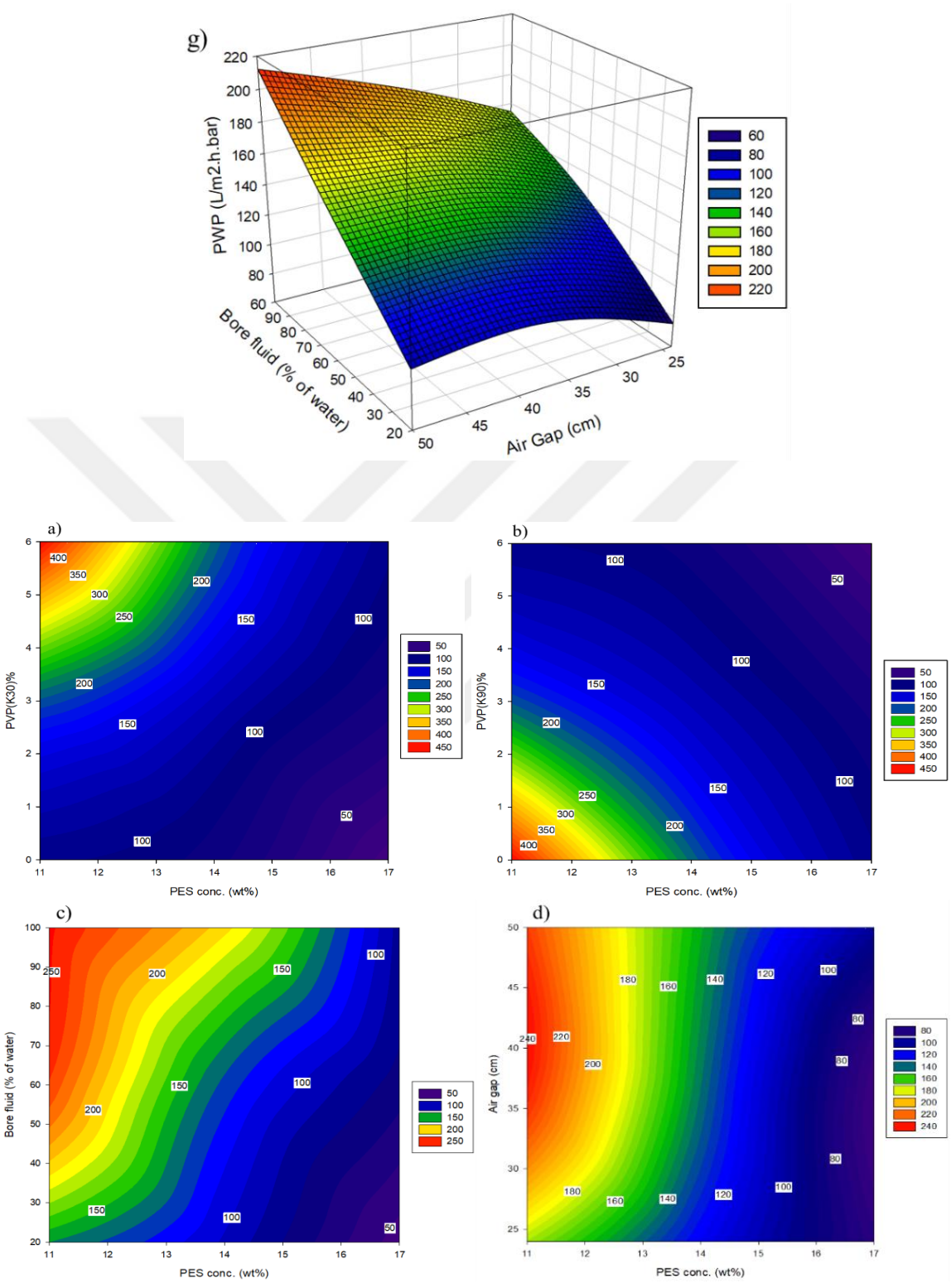
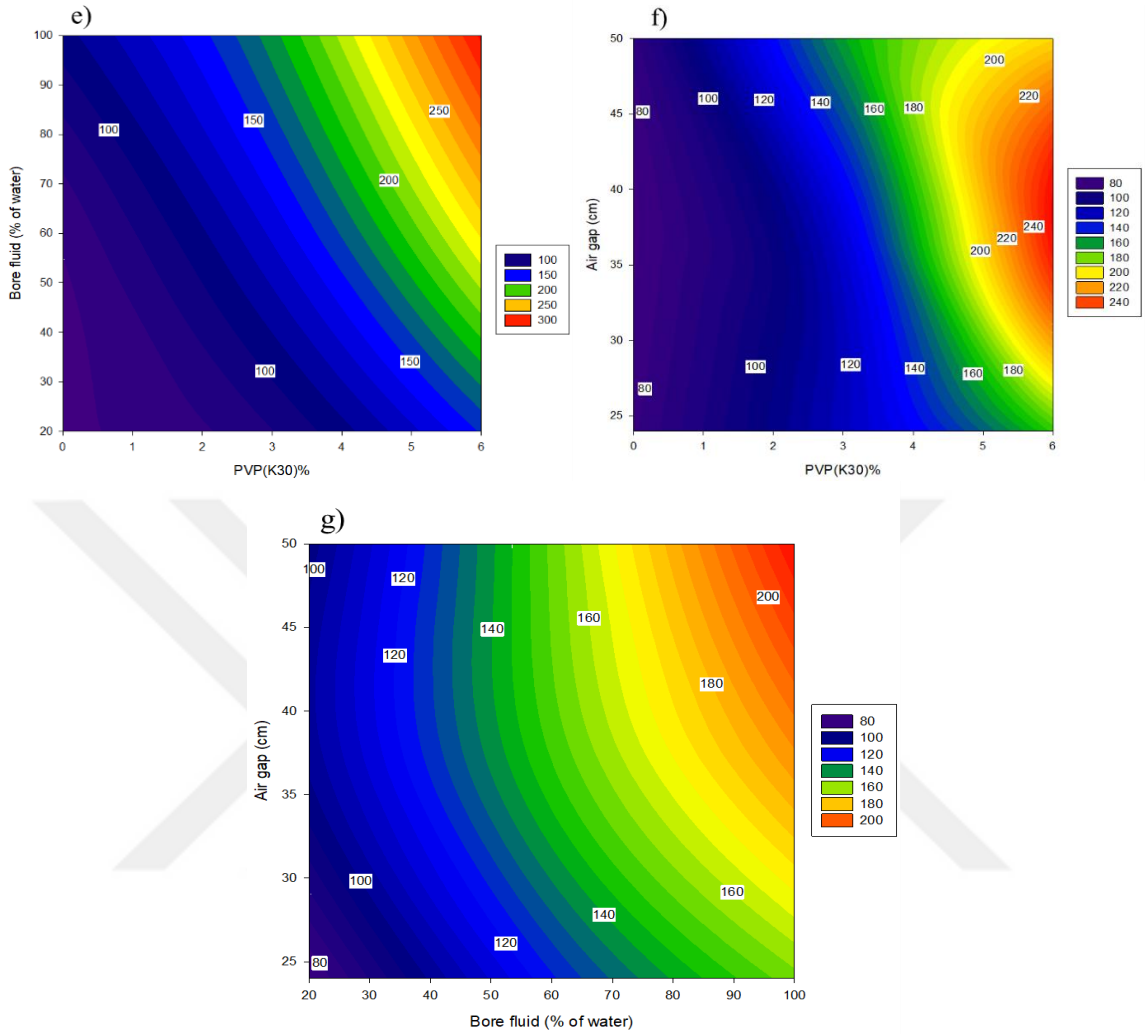


Figure 4.8. Contour plot of the variation of PWP in response to (a) polymer concentration and PVP (K30), (b) polymer concentration and PVP(K90), (c) polymer concentration and bore fluid, (d) polymer concentration and air gap, (e) PVP (K30) and bore fluid and (f) PVP (K30)

Figure 4.8. Continued



PVP is hydrophilic and hence improves the PWP of the membranes. However, since the overall concentration of PVP in the solution was kept constant at 6%, the effect of different molecular weights on the permeability was observed. Fig. 4.9 shows the variation of PWP as the K30:K90 ratio was changed. As observed from the figure, an increase in the concentration of K30 or a decrease in the concentration of K:90 increases the PWPof the membranes and vice versa. Fig. 4.7 and 4.8 show a 3D response surface plot and the contour plot of PWP as a function of PES concentration and K30:K90 concentration.

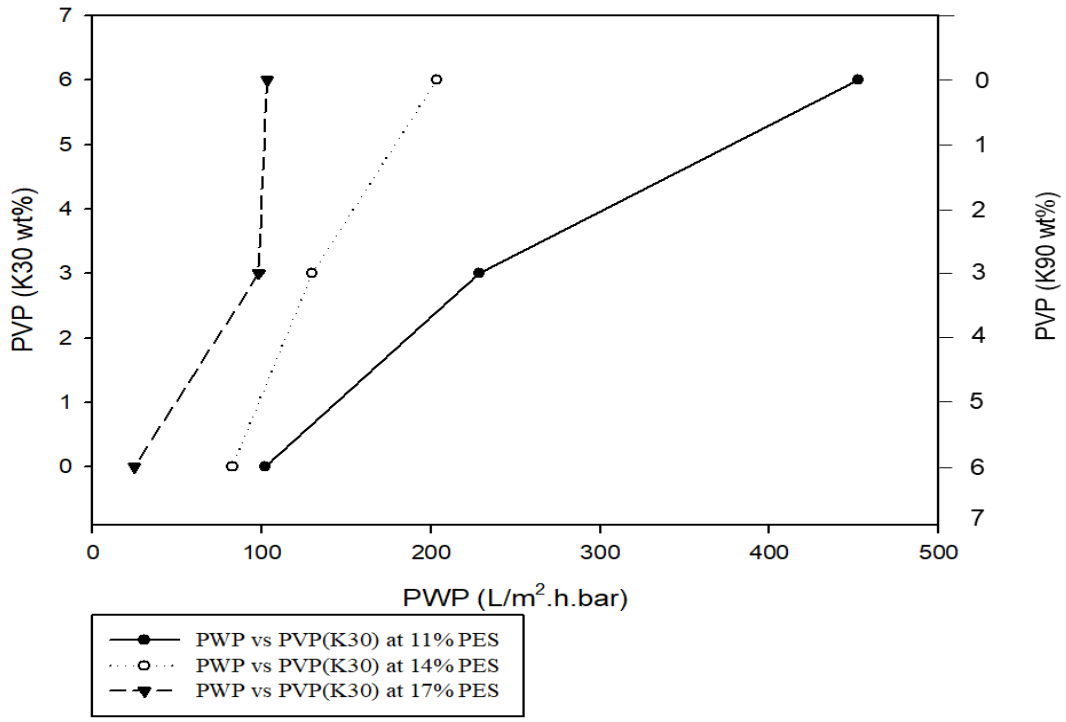


Figure 4.9. Change in PWP with PVP molecular weight

The design of experiment (DOE) statistical analysis generated a regression quadratic model equation for PWP as a function of the input variable (Equation 4.1).

$$PWP = 288 - 42.5z_1 + 92.2z_2 + 1.32z_3 + 1.77z_4 + 2.01z_1z_2 + 2.95z_2z_2 + 0.00456z_3z_3 + 0.0102z_4z_4 - 7.55z_1z_2 - 0.149z_1z_3 - 0.204z_1z_4 + 0.235z_2z_3 + 0.197z_2z_4 + 0.0170z_3z_4 \quad (4.1)$$

The analysis of variance (ANOVA) for the significance, fitness, and adequacy of PWP data was checked and is presented in Table 4.4.

Table 4.5. ANOVA output of the quadratic model for PWP.

ANOVA results for PWP					
Source	**DF**	**Adj SS**	**Adj MS**	**F-Value**	**P-Value**
Model	14	196380	14027,2	11,51	0
Linear	4	167759	41939,6	34,42	0
Z1	1	70045	70045,2	57,48	0
Z2	1	70533	70533,5	57,88	0
Z3	1	23859	23859,3	19,58	0,001
Z4	1	3321	3320,5	2,72	0,125

Table 4.4. Continued

Square	4	4867	1216,7	1	0,446
Z1*Z1	1	1741	1740,7	1,43	0,255
Z2*Z2	1	3762	3762,2	3,09	0,104
Z3*Z3	1	284	284,3	0,23	0,638
Z4*Z4	1	16	15,8	0,01	0,911
2-Way Interaction	6	23755	3959,1	3,25	0,039
Z1*Z2	1	18479	18479	15,16	0,002
Z1*Z3	1	1279	1279,4	1,05	0,326
Z1*Z4	1	254	254,3	0,21	0,656
Z2*Z3	1	3192	3192,5	2,62	0,132
Z2*Z4	1	235	235,2	0,19	0,668
Z3*Z4	1	314	314,4	0,26	0,621
Error	12	14623	1218,6		
Lack-of-Fit	10	14330	1433	9,75	0,096
Pure Error	2	294	146,9		
Total	26	211003			

As seen in Table 4.4, the F-values are large indicating that the model is significant. On the other hand, P-values if less than 0.05 are deemed significant. Hence, Z1, Z2, and Z3 i.e., PES concentration, PVP molecular weight, and bore fluid are more important and effective factors in comparison to the air gap. Also, the interaction between the factors can only be observed between PES concentration and PVP molecular weight. The interaction between other parameters is not significant due to their P-values being greater than 0.05. Pareto chart (Figure 4.10) visual representation of various factors and their significance.

Table 4.6. Model summary of R^2

Model Summary		
S	**R-squared**	**R-sq(adj)**
34,9086	93,07%	84,98%

The value of R^2 for the PWP is 93.1%. This indicates that only 6.93,% of the PWP data from the experiments cannot be explained by using the current model. Also, the R^2-adjusted value of 85% is adequately high.

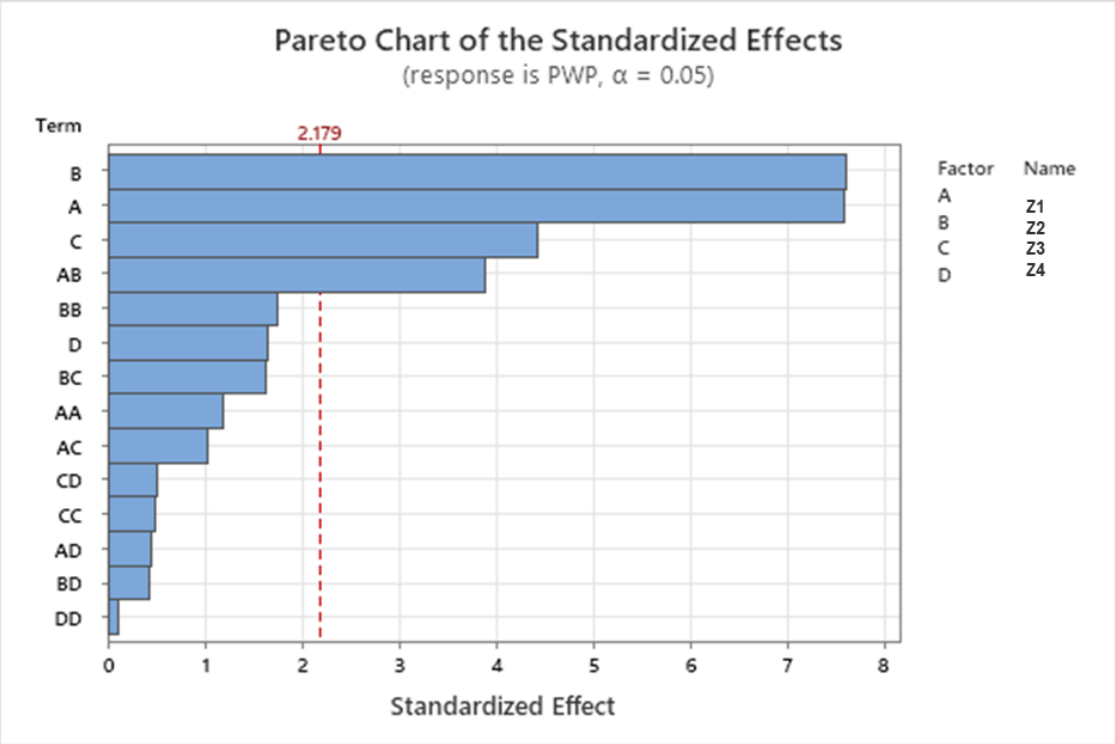


Figure 4.10. Visual representation of the significance of various spinning factors on PWP

4.6. Effect of Various Parameters on Porosity of The Produced Samples

The term “Porosity” is the measurement of the void space inside a membrane's structure. Because the pores in the membrane support layer are larger than those in the membrane skin layer, the structure of the membrane support layer has a greater impact on membrane porosity [61]. Feng et. al used the phase inversion process to prepare flat sheet poly (vinylidene fluoride-co-tetrafluoroethylene) membranes using DMA as the bore fluid and $LiClO_4 \cdot 3H_2O$ and TMP as the additives [62]. They demonstrated that with increasing polymer concentration, the porosity of poly (vinylidene fluoride-co-tetrafluoroethylene) membrane decreased.

Research by Khayet et al., while testing a variety of PVC polymer concentrations (14-20%), the addition of PVP or PEG additives improved the properties of PVC membranes [63]. An increase in the porosity of the fiber was reported. The effect of the spinning parameters on the porosity of hollow fiber membranes in the current study is in agreement with the existing literature. Figures 4.11 a) to g) and Figure 4.12 a) to g) shows the variation of the porosity as 3-dimensional response surface plots and contour plots with varying input parameters.

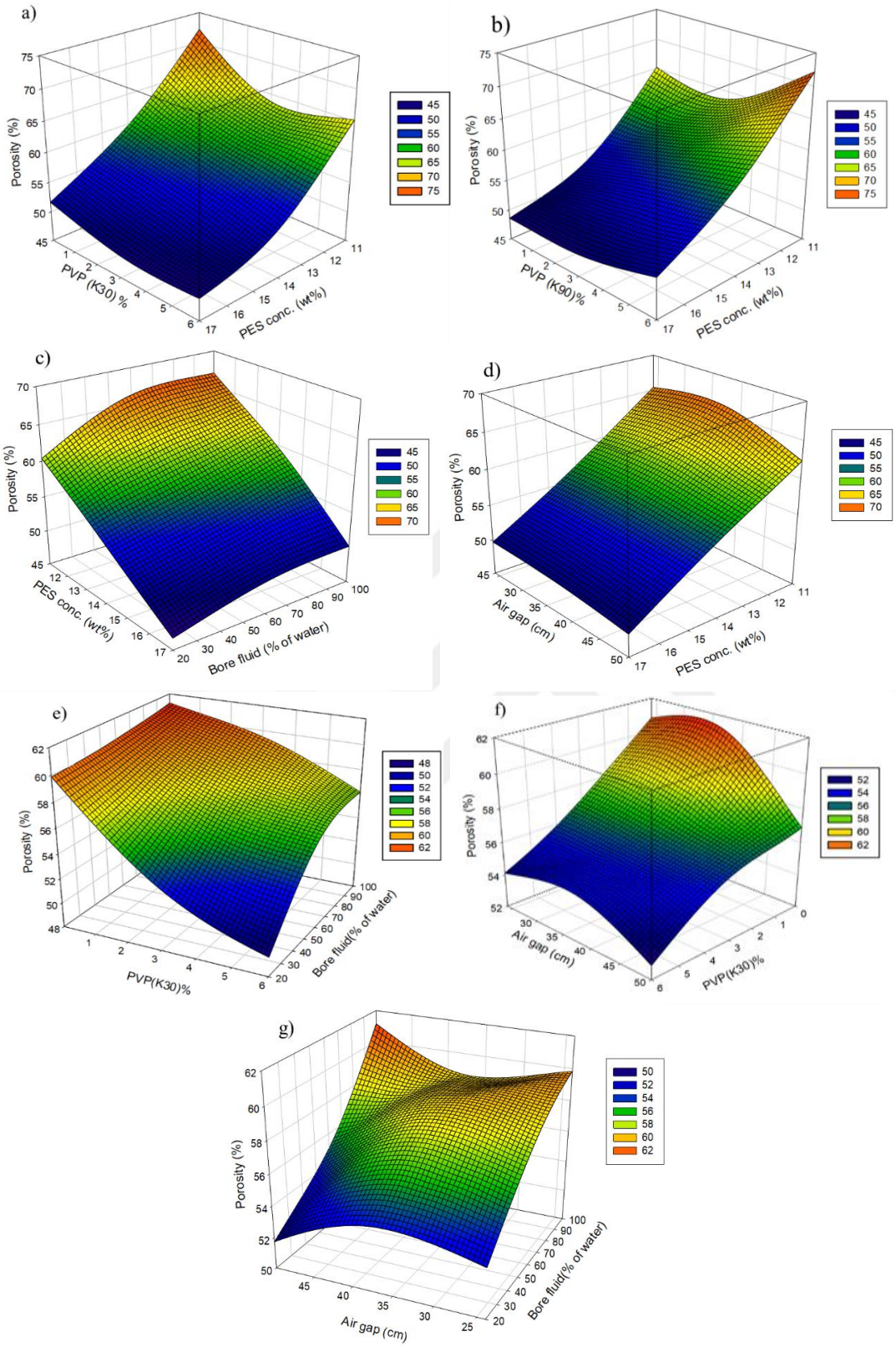


Figure 4.11. 3-dimensional response surface plot for porosity in response to (a) polymer concentration and PVP (K30), (b) polymer concentration and PVP (K90), (c) polymer concentration and bore fluid, (d) polymer concentration and air gap, (e) PVP (K30) and bore fluid, (f) PVP (K30) and air gap and (g) bore fluid and air gap.

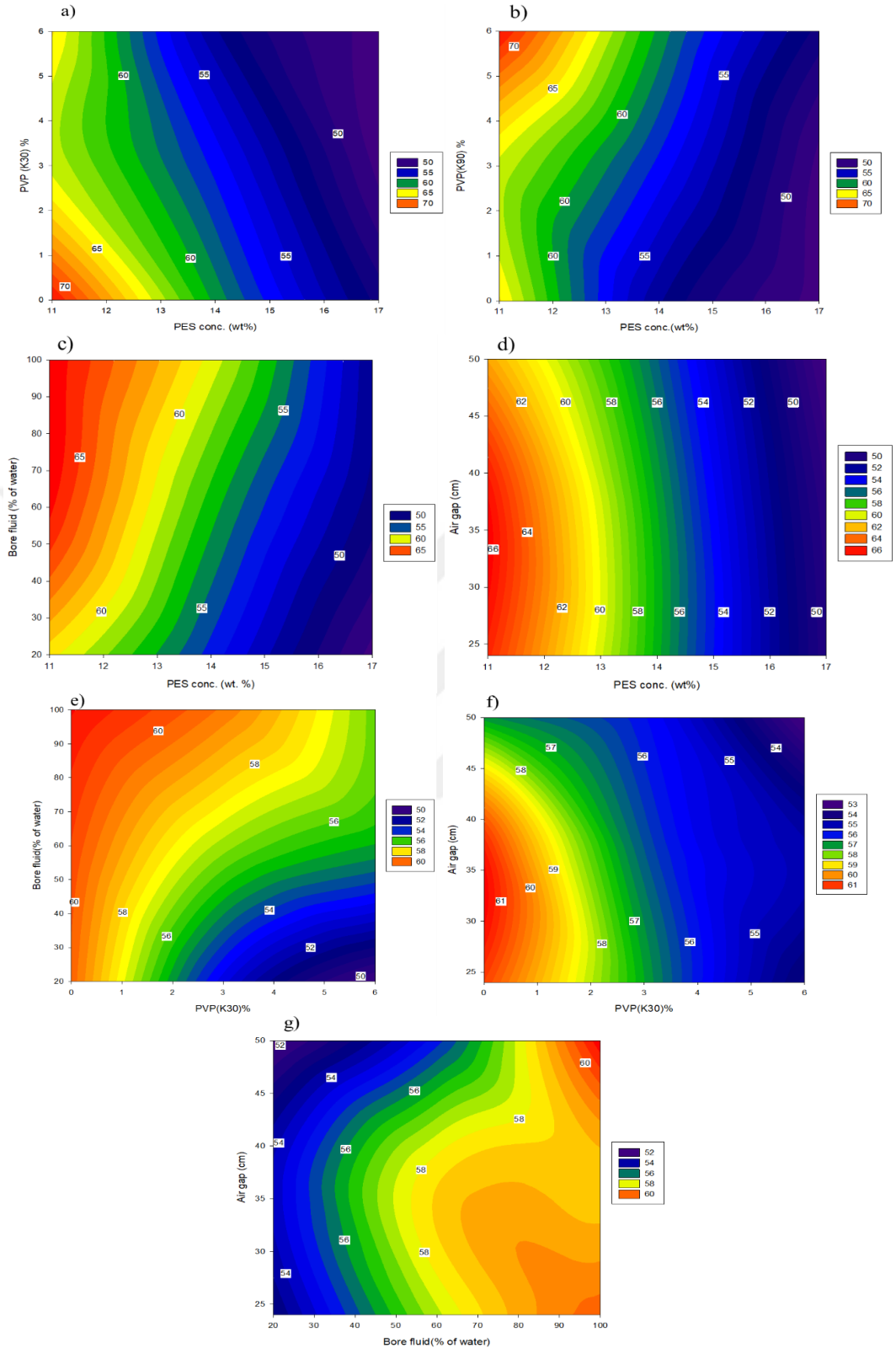


Figure 4.12. Contour plot of the variation of porosity in response to a) polymer concentration and PVP (K30), b) polymer concentration and PVP(K90), c) polymer concentration and bore fluid, d) polymer concentration and air gap, e) PVP (K30) and bore fluid, f) PVP (K30) and air gap, g) bore fluid and air gap.

The design of experiment (DOE) regression quadratic model equation for porosity as a function of the input variable is given in Equation 4.2 below.

$$Porosity = 115.4 - 5.93z_1 - 2.30z_2 + 0.146z_3 + 0.133z_4 + 0.115z_1z_1 + 0.142z_2z_2 - 0.000598z_3z_3 - 0.00623z_4z_4 - 0.049z_1z_2 - 0.0060z_1z_3 + 0.0096z_1z_4 + 0.0109z_2z_3 + 0.0168z_2z_4 + 0.00132z_3z_4 \quad (4.2)$$

The analysis of variance (ANOVA) for the significance, fitness, and adequacy of the porosity was checked and is presented in Table 4.6.

Table 4.7. ANOVA output of the quadratic model for the porosity

ANOVA for Porosity					
Source	**DF**	**Adj SS**	**Adj MS**	**F-Value**	**P-Value**
Model	14	1119,73	79,981	10,86	0
Linear	4	1068,05	267,012	36,27	0
Z1	1	885,29	885,285	120,25	0
Z2	1	77,83	77,826	10,57	0,007
Z3	1	96,79	96,787	13,15	0,003
Z4	1	8,15	8,151	1,11	0,313
Square	4	37,75	9,438	1,28	0,331
Z1*Z1	1	5,71	5,713	0,78	0,396
Z2*Z2	1	8,76	8,755	1,19	0,297
Z3*Z3	1	4,88	4,877	0,66	0,432
Z4*Z4	1	5,91	5,908	0,8	0,388
2-Way Interaction	6	13,93	2,321	0,32	0,917
Z1*Z2	1	0,77	0,766	0,1	0,753
Z1*Z3	1	2,1	2,103	0,29	0,603
Z1*Z4	1	0,56	0,563	0,08	0,787
Z2*Z3	1	6,89	6,891	0,94	0,352
Z2*Z4	1	1,72	1,716	0,23	0,638
Z3*Z4	1	1,89	1,891	0,26	0,622
Error	12	88,34	7,362		
Lack-of-Fit	10	83,99	8,399	3,86	0,223
Pure Error	2	4,35	2,176		
Total	26	1208,07			

The F-values for porosity in Table 4.6 is again large. Hence the porosity model is considered significant. The P-values are less than 0.05 for three out of four parameters. Hence, Z1, Z2, and Z3 i.e., PES concentration, PVP molecular weight, and bore fluid are more important and effective factors in comparison to the air gap. Also, no interaction is found between any of the factors. Hence, the effect of factor interactions is deemed to be insignificant due to their P-values being greater than 0.05 for porosity. Pareto chart (Figure 4.13) visual representation of various factors and their significance.

Table 4.8. Model summary of R^2 for porosity

Model Summary		
S	**R-sq**	**R-sq(adj)**
2,71328	92,69%	84,16%

The value of R^2 for the porosity is 92.7%. This indicates that only 7.3% of the porosity data from the experiments cannot be explained by using the current model. Also, R^2-adjusted value of 84.2% is sufficiently high.

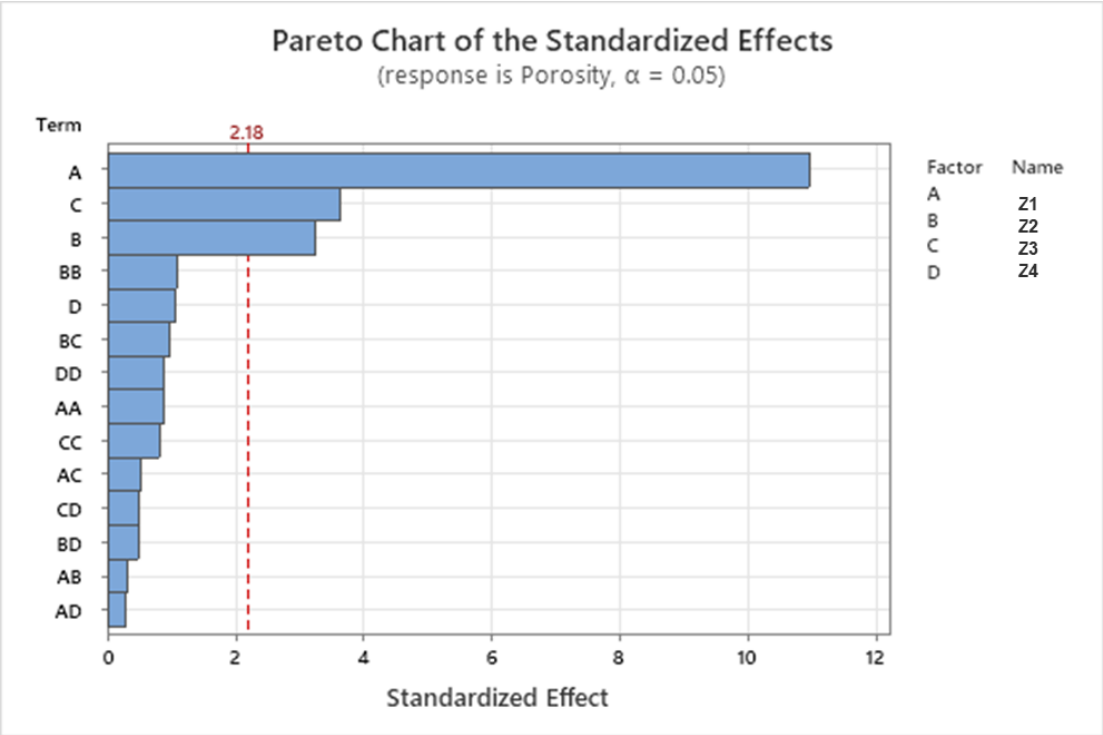


Figure 4.13. Visual representation of the significance of various spinning factors on porosity

4.7. Pore Size Variation

There is a wide range of fluctuation in the pore sizes of the fabricated hollow fiber membranes. Fibers with spongy structures have smaller pore sizes while the fibers with finger-like intrusion cells have larger pore sizes. As an example, a comparison between the pore sizes of the sample with the highest permeability (E16; PES = 11%, PVP (K30) = 6%, BF =60:40, and AG = 37cm) and the sample with the lowest permeability (E5; PES = 17%, PVP (K90) = 6%, BF =60:40, and AG = 37cm) was done using ImageJ software and the results are shown in the Figure 4.14.

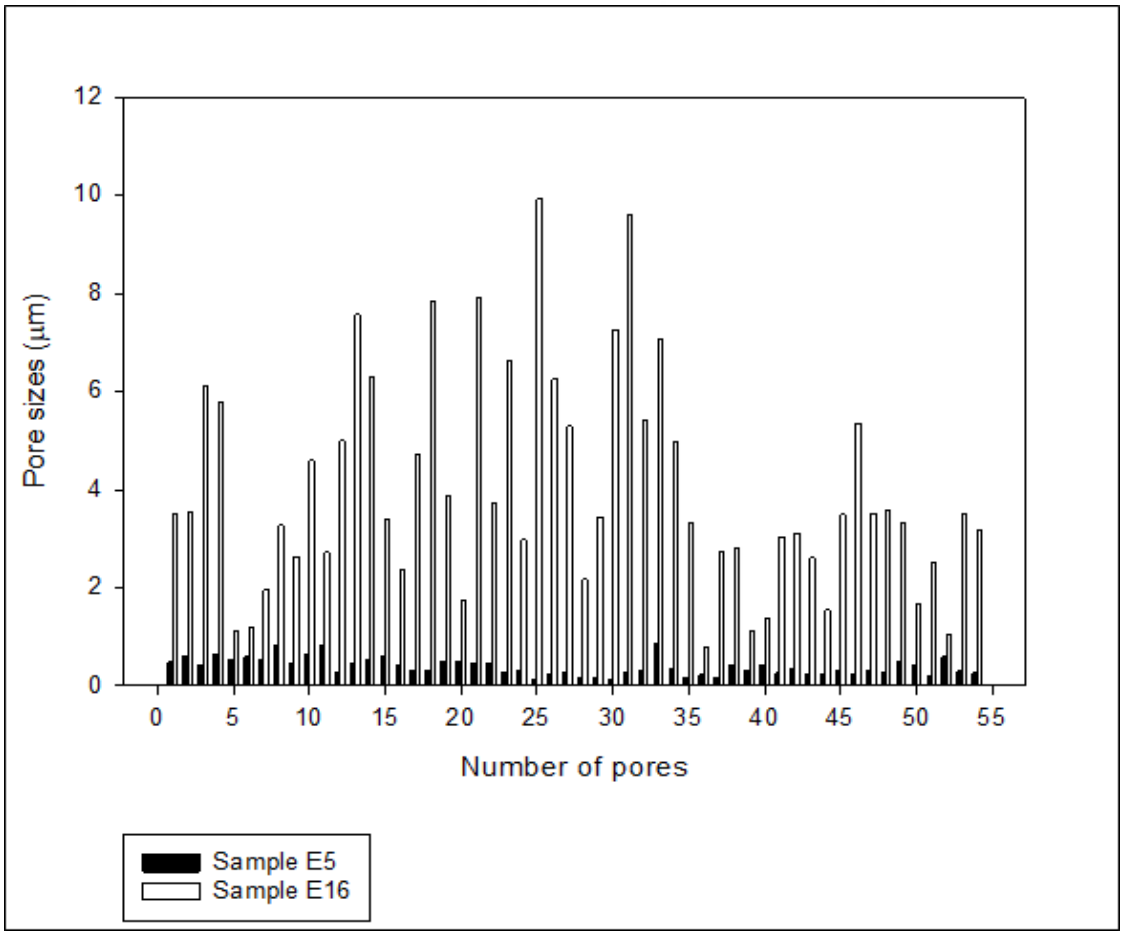


Figure 4.14. Pore size comparison between sample E5 and E16

The mean pore size for the sample E5 was 0.3869 µm while the mean pore size for sample E16 was 3.9883 µm i.e., almost 10 times the mean pore size of the sample E5 (Table 4.8).

Table 4.9. Pore size comparison between samples E5 and E16.

Sample	Mean pore size (µm)	Min. pore size (µm)	Max. pore size (µm)
E5	0.3869	0.1320	0.8560
E16	3.9883	0.7690	9.9300

In terms of morphology, samples E1, E23, and E25 showed asymmetric spongy structures. The pore sizes in these samples were small but varied along the radius. Figure 4.15 shows the average pore size variation through the wall thickness for sample E25.

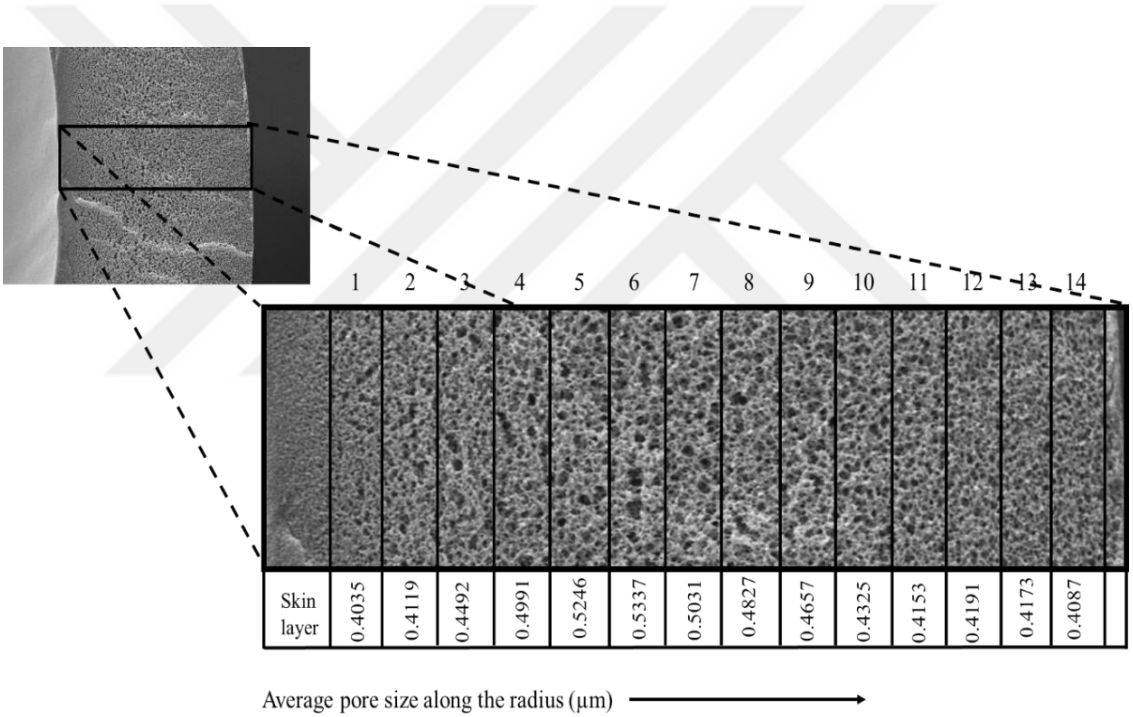


Figure 4.15. Average pore size distribution along the radius of sample E25

As seen from the figure, the pore sizes near the skin layer are quite small. These pores act as the demarcating factor for the largest solute particles that can pass through them. As we move radially outwards, there is a gradual increase in the average pore size until it reaches the mid-section. After that, the average pore sizes start to decrease (Figure 4.16). This could be caused by the compression of the membrane fiber while handling.

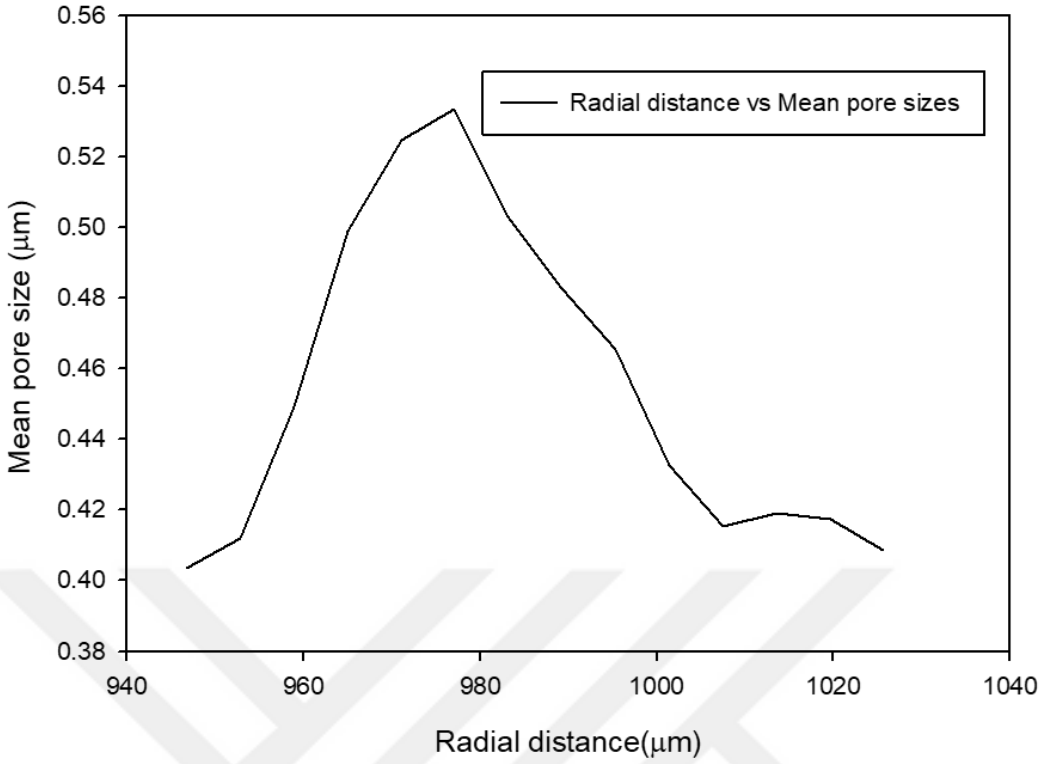


Figure 4.16. Average pore size distribution graph of sample E25

5. CONCLUSIONS AND RECOMMENDATIONS

5.1. Conclusions

Polyethersulfone (PES) hollow fiber membranes to be used in hemodialysis application were fabricated via phase inversion method in this study. To this end, an indigenously built setup was used to produce fibers. The fabricated membranes were then characterized. Pure water permeability, porosity, pore distribution, and morphology of the membranes were analyzed. The impacts of four major fabrication parameters, including PES concentration, PVP molecular weight, bore fluid composition, and air gap, on membrane structure, pure water permeability, porosity, and pore size distribution, were investigated using RSM and the Box–Behnken statistical model. The findings show that PES concentration and PVP molecular weights are important elements impacting membrane performance among the parameters tested. This research demonstrated that RSM is an effective method for optimizing the manufacture of PES/PVP membranes for maximal permeability and porosity. Following conclusions are made from the research.

1. Polymer concentration is a crucial parameter that affects the characteristics and morphology of membranes. Increasing the PES concentration leads to an increase in viscosity.
2. The pore sizes of the membranes for similar conditions reduced in size with an increase in PES concentration. This is due to the higher resistance to the diffusion of the non-solvent (water and alcohol in this case) into the polymer-rich phase resulting in finer pores.
3. Additives in the dope solution help infuse desired properties. Properties like hydrophilicity, permeability, rejection rate, and molecular weight cut-off (MWCO) can be fine-tuned by the use of additives.
4. Use of lower molecular weight PVP (K30 in this case) lead to the formation of intrusion cells while higher molecular weight PVP (K90 in this case) yielded spongy structures.
5. High miscibility, and high quenching power bore fluids create intrusion cells and macro voids. Water, as powerful quenching medium, leads to the formation of finger-like intrusion cells.

6. Rapid demixing between the bore fluid and the dope solution creates intrusion cells and macro voids while as slow demixing makes the membrane morphology spongy.
7. Air gap affects the wall thickness and the inner skin layer thickness. The wall thickness of the membranes increased from 64 µm to 77.2 µm, while the inner skin layer thickness increased from 1.6 µm to 3.1 µm respectively. Similarly, at 17% PES concentration, the wall thicknesses increased from 59.8 µm to 61µm and the corresponding inner skin layer thickness increased from 5.6 µm to 8.3 µm respectively.
8. PES concentration inversely affected the PWPof the membranes. The lowest permeability found was 24.781 l/m^2.h.bar at 17% polymer concentration while the highest permeability value found was 452.2 l/m^2.h.bar at 11% polymer concentration.
9. PES concentration, PVP molecular weight and bore fluid composition are significant factors affecting the properties of PES hollow fiber membranes. The air gap seems to have less significance on the properties of the membrane.

5.2. Recommendations

Even though the results of this study are important and in agreement with the previous works in the field of hemodialysis membranes. There is a lot of ground yet to be covered for this work to grow and reach a necessary conclusion. First of all, further tests like BSA rejection rate, molecular weight cut-off (MWCO), ultrafiltration coefficient, toxic clearances, etc. need to be performed. These tests will help expand the spectrum of underlying mechanisms of hemodialysis membranes.

The use of data-driven machine learning processes in the field of membrane technology has not yet been introduced as far as the conducted open literature survey. Training a machine to understand the effect of various parameters on the characteristics of the membranes and devising an algorithm to get the desired properties irrespective of the type of polymer, additive, or bore fluid used will make working with membranes much easier.

Lastly, new techniques like polymer blending, chemical modification, and biomimetic membrane production techniques to improve the bio and hemocompatibility of the membranes should be adopted. The polymer blending process is quite simple and less time-consuming. Adding chain extenders of different molecular weights (like PEG 600 and 2000 MW) has shown significant improvement in hemocompatibility and cytocompatibility.

The use of the state-of-the-art Zwitterionic structures has shown tremendous improvement in hemodialysis membranes. Biomimetic membrane techniques like bioadhesion and biomineralization are inspired by nature. A good example of such a membrane is heparin grafted membranes. Patients undergoing hemodialysis are administered heparin to prevent clotting of the blood. However, sometimes to reduce the risk of bleeding, heparin-free dialysis is required. So, membranes with immobilized grafted heparin on the blood side of the membrane are used.

6. REFERENCES

1. www.kidneyfund.org/kidney-disease/kidney-failure/ American Kidney Fund. 10 March 2022

2. Evans, R. W., Manninen, D. L., Garrison Jr, L. P., Hart, L. G., Blagg, C. R., Gutman, R. A., and Lowrie, E. G. The quality of life of patients with end-stage renal disease, New England Journal of Medicine, 312, 9 (1985) 553-559.

3. Medical Uses of Water Figure Showing Hemodialysis Process, https://www.cdc.gov/healthywater/other/medical/hemodialysis_process_fig.html 2022.

4. Jha, V., Garcia-Garcia, G., Iseki, K., Li, Z., Naicker, S., Plattner, B., and Yang, C. W. Chronic kidney disease: global dimension and perspectives, The Lancet, 382, 9888 (2013) 260-272.

5. https://pharm.ucsf.edu/kidney/need/statistics The Kidney Project. 20 March 2022

6. Seyahi, N., Ateş, K., and Süleymanlar, G. Current Status of Renal Replacement Therapy in Turkey: A Summary of the Turkish Society of Nephrology Registry Report. Current Status of Renal Replacement Therapy in Turkey, 2020.

7. Said, N., Lau, W. J., Ho, Y. C., Lim, S. K., Zainol Abidin, M. N., and Ismail, A. F. A review of commercial developments and recent laboratory research of dialyzers and membranes for hemodialysis application, Membranes, 11,10 (2021) 767.

8. Bottino A., Camera-Roda, G., Capannelli, G. and Munari, S, "The formation of microporous polyvinylidene difluoride membranes by phase separation," Journal of Membrane Science, (1991) 1-20.

9. Feng C., Khulbe K., Matsuura T., and Ismail A., Recent progresses in polymeric hollow fiber membrane preparation, characterization and applications, Separation and Purification Technology, 111 (2013) 43-71.

10. Xiao K., Liang S., Wang X., Chen C., and Huang X., "Current state and challenges of full-scale membrane bioreactor applications: A critical review," Bioresource Technology, 271, (2019) 473-481.

11. Klaassen R., Feron P., and Jansen A., Membrane contactors in industrial applications, Chemical Engineering Research and Design, 83, (2005) 234-246.

12. https://synderfiltration.com/learning-center/articles/introduction-to-membranes/definition-of-a-membrane/ Synder Filtration 20 March 2022.

13. Sujata V. Bhat, Second edition page no. 1. Biomaterials Second Edition. New Delhi: Narosa Publishing House, 2007.

14. Haemodialysis membranes. Ronco, Claudio and Clark, William R. June, s.l. : Macmillan Publishers Limited, part of Springer Nature, 14, (2018) 394-410.

15. https://www.freseniusmedicalcare.com/en/media/insights/company-features/ the-history-of-dialysis/ The history of dialysis, 21 March 2022

16. Cameron, J. S. A history of the treatment of renal failure by dialysis, 2002.

17. Di Paola, L. Artificial kidney: A chemical engineering challenge. In Current Trends and Future Developments on (Bio-) Membranes, Elsevier, (2020) 1-20.

18. https://www.homedialysis.org/home-dialysis-basics/machines-and-supplies/ dialysis-museum#prettyPhoto Dialysis machnine museum, 21 March 2022.

19. Twardowski, Z. J., History of hemodialyzers' designs. Hemodialysis International, 12,2 (2008) 173-210.

20. Warsinger D. M., Chakraborty S., Tow E. W., Plumlee M. H., Bellona C., Loutatidou S., et al., A review of polymeric membranes and processes for potable water reuse, Progress in Polymer Science, 81, (2018) 209-237.

21. Eduok U., Abdelrasoul A., Shoker A., and Doan H., Recent Developments, Current Challenges and Future Perspectives on Cellulosic Hemodialysis Membranes for Highly Efficient Clearance of Uremic Toxins, Materials Today Communications, (2021) 102183.

22. Dehban, A., Saeedavi, F. H., & Kargari, A. A study on the mechanism of pore formation through VIPS-NIPS technique for membrane fabrication, Journal of Industrial and Engineering Chemistry, 108, (2022) 54-71.

23. Rajabzadeh, S., Maruyama, T., Ohmukai, Y., Sotani, T., and Matsuyama, H. Preparation of PVDF/PMMA blend hollow fiber membrane via thermally induced phase separation (TIPS) method, Separation and Purification Technology, 66,1 (2009) 76-83.

24. Mat Nawi, N. I., Chean, H. M., Shamsuddin, N., Bilad, M. R., Narkkun, T., Faungnawakij, K., & Khan, A. L. Development of hydrophilic PVDF membrane using vapour induced phase separation method for produced water treatment, Membranes, 10,6 (2020) 121.

25. Zhao, J., Luo, G., Wu, J., and Xia, H. Preparation of microporous silicone rubber membrane with tunable pore size via solvent evaporation-induced phase separation, ACS Applied Materials & Interfaces, 5, 6 (2013) 2040-2046.

26. Wnek G. E., Carr M. E., Simpson D. G., and Bowlin G. L., Electrospinning of nanofiber fibrinogen structures, Nano letters, 3 (2003) 213-216.

27. Su C., Li Y., Cao H., Lu C., Li Y., Chang J., et al., Novel PTFE hollow fiber membrane fabricated by emulsion electrospinning and sintering for membrane distillation, Journal of Membrane Science, 583, (2019) 200-208.

28. Anka F. H. and Balkus(Jr) K. J., Novel nanofiltration hollow fiber membrane produced via electrospinning, Industrial & Engineering Chemistry Research, 52, (2013) 3473-3480.

29. Tan X. and Rodrigue D., A review on porous polymeric membrane preparation. Part I: production techniques with polysulfone and poly (vinylidene fluoride), Polymers, 11, (2019) 1160.

30. Toimil-Molares M. E., Characterization and properties of micro-and nanowires of controlled size, composition, and geometry fabricated by electrodeposition and ion-track technology, Beilstein Journal of Nanotechnology, 3 (2012) 860-883.

31. Abdullah N., Rahman M. A., Othman M. H. D., Ismail A., Jaafar J., and Abd Aziz A., Preparation and characterization of self-cleaning alumina hollow fiber membrane using the phase inversion and sintering technique, Ceramics International, 42, (2016) 12312-12322.

32. Bărdacă Urducea C., Nechifor A. C., Dimulescu I. A., Oprea O., Nechifor G., Totu E. E., et al., Control of Nanostructured Polysulfone Membrane Preparation by Phase Inversion Method, Nanomaterials, 10 (2020) 2349.

33. Wang D.-M. and Lai J.-Y., Recent advances in preparation and morphology control of polymeric membranes formed by nonsolvent induced phase separation, Current Opinion in Chemical Engineering, 2 (2013) 229-237.

34. Guillen G. R., Pan Y., Li M., and Hoek E. M., Preparation and characterization of membranes formed by nonsolvent induced phase separation: a review, Industrial & Engineering Chemistry Research, 50 (2011) 3798-3817.

35. Kim J. F., Kim J. H., Lee Y. M., and Drioli E., Thermally induced phase separation and electrospinning methods for emerging membrane applications: A review, AIChE Journal, 62 (2016) 461-490.

36. Zeinali R., Del Valle L. J., Torras J., and Puiggalí J., Recent progress on biodegradable tissue engineering scaffolds prepared by thermally-induced phase separation (Tips), International Journal of Molecular Sciences, 22 (2021) 3504.

37. Park H. C., Kim Y. P., Kim H. Y., and Kang Y. S., Membrane formation by water vapor induced phase inversion, Journal of Membrane Science, 156 (1999) 169-178.

38. Mat Nawi N. I., Chean H. M., Shamsuddin N., Bilad M. R., Narkkun T., Faungnawakij K., et al., Development of hydrophilic PVDF membrane using vapour induced phase separation method for produced water treatment, Membranes, 10 (2020) 121.

39. https://www.onlinetextileacademy.com/dry-spinning-process-advantagesand-disadvantages-of-dry-spinning/ 21 March 2022

40. https://textilelearner.net/principle-and-uses-of-wet-spinning/ 22 March 2022

41. https://www.nal.res.in/en/techniques/dry-jet-wet-fiber-spinning-technique 25 March 2022

42. https://secant.com/technology/custom-fiber-extrusion-technology/fiber-extrusion-capabilities 25 March 2022

43. Bildyukevich A. V., Plisko T. V., and Usosky V. V., The Formation of Polysulfone Hollow Fiber Membranes by the Free Fall Spinning Method, Petroleum Chemistry, 56 (2016) 379–400.

44. Chung T. S., Qin J. J., and Gu J., Effect of shear rate within the spinneret on morphology, separation performance and mechanical properties of ultrafiltration polyethersulfone hollow fiber membranes, Chemical Engineering Science, 55 (2000) 1077-1091.

45. Bakeri G., Ismail A. F., Shariaty-Niassar M., and Matsuura T., Effect of polymer concentration on the structure and performance of polyetherimide hollow fiber membranes, Journal of Membrane Science, 363 (2010)103-111.

46. Sengur R., Turken T., Wiesner M., and Koyuncu I., Fabrication and characterization of hydroxylated and carboxylated multiwalled carbon nanotube/polyethersulfone (PES) nanocomposite hollow fiber membranes, Desalination, (2015) 123-140.

47. Cabasso, I., Klein, E., and Smith, J. K. Polysulfone hollow fibers. I. Spinning and properties, Journal of Applied Polymer Science, 20,9 (1976) 2377-2394.

48. Xu Z. L. and Qusay F. A., Effect of polyethylene glycol molecular weights and concentrations on polyethersulfone hollow fiber ultrafiltration membranes, Journal of Applied Polymer Science, 91 (2004) 3398-3407.

49. https://polymerdatabase.com/Polymer%20Brands/PES.html 30 April 2022

50. https://www.chemicalbook.com/ChemicalProductProperty_EN_CB4209342.htm 30 April 2022.

51. Kang, B., Li, Y. D., Liang, J., Yan, X., Chen, J., and Lang, W. Z. Novel PVDF hollow fiber ultrafiltration membranes with antibacterial and antifouling properties by embedding N-halamine functionalized multi-walled carbon nanotubes (MWNTs), RSC Advances, 6(3) (2016) 1710-1721.

52. Alsalhy, Q. F., Salih, H. A., Simone, S., Zablouk, M., Drioli, E., & Figoli, A. Poly (ether sulfone) (PES) hollow-fiber membranes prepared from various spinning parameters, Desalination, 345 (2014) 21-35.

53. Liu, X., Liu, H., and Li, P. Effect of polymer dope concentration on the morphology and performance of PES/PDMS hollow fiber composite membrane for gas separation, PES, 500,28 (2017), 72.

54. Naim, R. and Ismail, A. F., Effect of polymer concentration on the structure and performance of PEI hollow fiber membrane contactor for CO_2 stripping, Journal of Hazardous Materials, 250, (2013) 354-361.

55. Xu, Z. L., Chung, T. S., & Huang, Y. U. Effect of polyvinylpyrrolidone molecular weights on morphology, oil/water separation, mechanical and thermal properties of polyetherimide/polyvinylpyrrolidone hollow fiber membranes, Journal of Applied Polymer Science, 74,9 (1999) 2220-2233.

56. Otitoju, T. A., Ahmad, A. L., & Ooi, B. S. Influence of ethanol as bore fluid component on the morphological structure and performance of PES hollow fiber membrane for oil in water separation, Korean Journal of Chemical Engineering, 34,10 (2017) 2703-2709.

57. Ahmad, A. L. and Shafie, Z. M. H. M., Effect of Air Gap Distance on PES/PVA Hollow Fibre Membrane's Morphology and Performance, Journal of Physical Science, 28 (2017).

58. Bakeri, G., Ismail, A. F., Shariaty-Niassar, M., and Matsuura, T. Effect of polymer concentration on the structure and performance of polyetherimide hollow fiber membranes, Journal of Membrane Science, 363,1-2 (2010)103-111.

59. Eren, B & Güney, M., The role of polyvinylpyrrolidone as a pore former on microstructure and performance of polysulfone membranes, Bilecik Şeyh Edebali Üniversitesi Fen Bilimleri Dergisi. 6 (2019) 168-176

60. Shi, L., Wang, R., Cao, Y., Liang, D. T., & Tay, J. H. Effect of additives on the fabrication of poly (vinylidene fluoride-co-hexafluropropylene)(PVDF-HFP) asymmetric microporous hollow fiber membranes, Journal of Membrane Science, 315,1-2, (2008) 195-204.

61. Bakeri, G., Ismail, A. F., DashtArzhandi, M. R., and Matsuura, T. Porous PES and PEI hollow fiber membranes in a gas–liquid contacting process - A comparative study, Journal of Membrane Science, 475 (2015) 57-64.

62. Feng, C., Shi, B., Li, G., and Wu, Y. Preparation and properties of microporous membrane from poly (vinylidene fluoride-co-tetrafluoroethylene) (F2. 4) for membrane distillation, Journal of Membrane Science, 237,1-2 (2004) 15-24.

CURRICULUM VITAE

He attained his First School Leaving Certificate in 2003. He is an alumnus of the prestigious Kashmir University. He earned a Bachelor of Engineering Degree in Mechanical Engineering in 2016 with the thesis titled “Use of Drones in Agriculture”. In 2018 he won the Turkiye Scholarship which presented him with the opportunity to study Master of Science in Mechanical Engineering at the prestigious Karadeniz Technical University. He did a year of the Turkish language course and resumes for the MSc program in 2019. Adil speaks English, Urdu, Hindi, Kashmiri and Turkish. Adil is currently enrolled in the program with the hope to round up in July 2022